Scientific Report

2011-2016

The activities taking place during the present project were focused on the analysis of experimental data obtained using ALICE experimental device at LHC-CERN in p-p collisions at 7 TeV and phenomenological models predictions for their interpretation.

- ***Light flavor hadron spectra and search for collective phenomena in high multiplicity pp collisions measured in the ALICE experiment.***

Introduction

Transverse momentum spectra of identified charged hadrons in p+p(pbar) collisions were studied as a function of incident energy below 900 GeV at CERN ISR and SppS and up to 1800 GeV at Fermilab Tevatron colliders. While UA5 Collaboration reported, starting from 200 GeV, an increase of $< p_T >$ of kaons in the central region larger than that expected based on ISR data, the E735 Collaboration evidenced a mass dependent slope of $<p_T>$ as a function of c.m. energy from 300 to 1800 GeV. Definitely such trend which significantly deviates from a ln(s) extrapolation from lower energies measured at ISR cannot be explained by models based on statistical equilibrium. Detailed studies of E735 Collaboration at 1800 GeV have shown that the increase of $<p_T>$ with $dNc/d\eta$ depends on the particle mass.

These studies are of real interest for different QCD inspired models like EPOS which predicts such a dependence as a consequence of a hydrodynamic type evolution with flux tube initial conditions. CDF Collaboration, comparing two energies, i.e. 630 GeV and 1800 GeV, evidenced an energy invariance of the p_T distribution at fixed multiplicity for soft interactions. This shows that the multiplicity of produced particles is a measure of the amount of energy involved in the process. Such a conclusion is supported by recent low relative momentum two-pion correlation studies at 0.9 and 7 TeV which evidenced that the correlation functions at the two energies are similar at a given multiplicity, the size of the emitting system growing with the charged particle multiplicity of the event. It was also evidenced that double and triple partonic interactions start to be significant at higher energies and their cross sections seem to increase linearly with ln(s), where s is the energy in the center of mass of the colliding system.
At about 4 times larger incident energies, as is the case of the present study, such processes contribute to a large energy transfer in the collision volume of proton size which could be well thermalized if we consider the mean free path of $0.2 - 0.3$ fm derived from QGP viscosity and that two – three collisions are in principle sufficient for thermalization. Therefore is quite probable that at such energies, a piece of matter of proton size, with a radius a few times larger (2.5-4.5) than the mean free path, hydrodynamically explodes if enough energy is produced inside.
In order to evidence such phenomena, a detailed analysis of transverse momentum distributions for high multiplicity and close to azimuthal isotropy events is required.
Multiplicity is defined as the number of charged particles in a given pseudorapidity range. The pseudorapidity range used for the multiplicity and the event shape analysis is $|\eta| < 0.8$ in the studies described below.

a. Studies as a function of multiplicity

Light flavor hadron spectra have been obtained for pp collisions at 7 TeV as a function of multiplicity. Therefore, detailed studies on the corrections and their multiplicity dependence, which have to be applied to the raw transverse momentum spectra for charged particles and identified hadrons for obtaining the primary spectra, namely:

- the reconstruction efficiency of the charged particle trajectories
- the matching efficiency in position between the TPC and TOF detectors
- the multiplicity dependence of the efficiency correction
- the particle identification strategy, PID efficiency and contamination
- the estimation of transverse momentum distributions contamination from weak decays and secondary interactions with the detector material
- the trigger and vertex reconstruction efficiencies

followed by:

- the extension of the kaon pT distribution range and validation of the Bayesian PID method
- the successful comparison with MB p spectra obtained using the nσ and unfolding methods

and the systematic errors estimate, coming from:

- trajectory reconstruction
- the receipt for obtaining the input probabilities in the Bayesian identification method
- contaminations coming from the neighboring hadron species
- the identification efficiency
- the secondary particles

were done, some of them being described in the previous reports.
The multiplicity selector used was also an issue of debate, combined multiplicity and forward detectors, V0M selectors being the two options in the multiplicity dependent spectra construction.

In Fig. 1 final transverse momentum spectra for charged particles obtained in nine combined multiplicity ranges are presented.

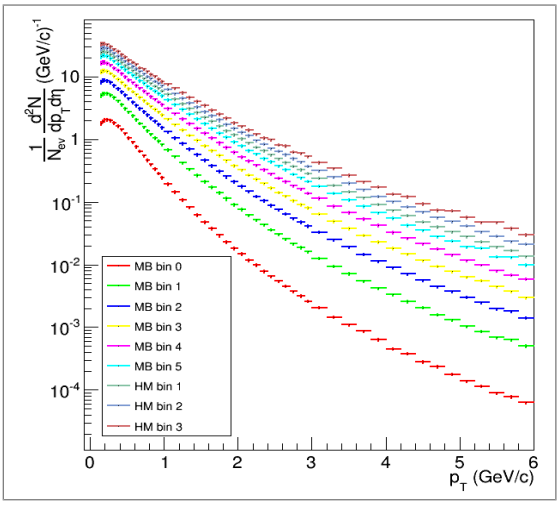

Fig. 1

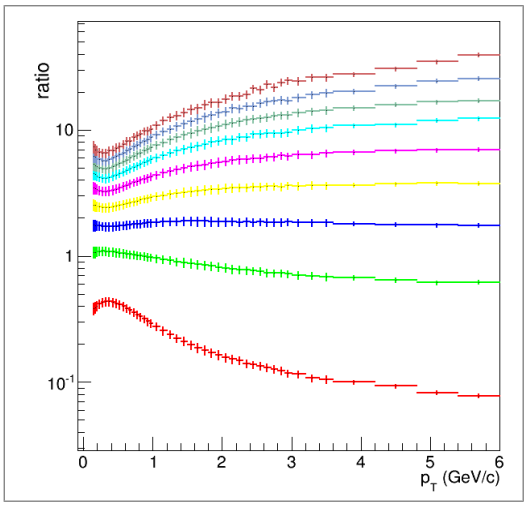

Fig. 2

The ratios between the transverse momentum spectra for different multiplicities relative to the non-conditioned spectrum in the charged particle multiplicity are presented in Fig. 2. A decrease of the ratio at small values of the transverse momentum can be observed, which enhances with increasing multiplicity, followed by an increase up to pT values around 2.5 GeV/c after which the increase has a very small slope suggesting a saturation at values of the transverse momentum larger than 6 GeV/c. The decrease of the ratios at small values of the transverse momentum which enhances with increasing multiplicity, seems to indicate the existence of a collective type expansion.
In order to obtain the average value of the transverse momentum $<p_T>$, the experimental spectra

were fitted with different expressions (described below) suggested by phenomenological models as modified Hagedorn, Levy-Tsallis, UA1 and a combination between a Boltzmann type exponential distribution and a power-law in the transverse momentum suggested by Bylinkin et al. The best fits were obtained using the last expression. Thus, the extrapolation of the experimental spectra at smaller values than the measured ones of the transverse momentum was done based on the fits performed with this expression. The obtained results for <pT> in the chosen multiplicity intervals are presented in Fig. 3.

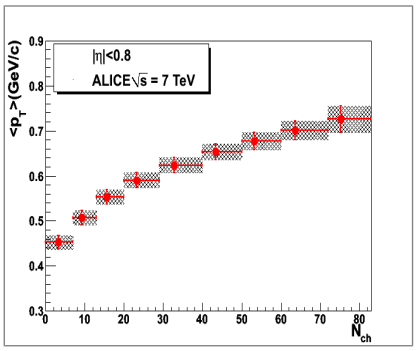

Fig. 3

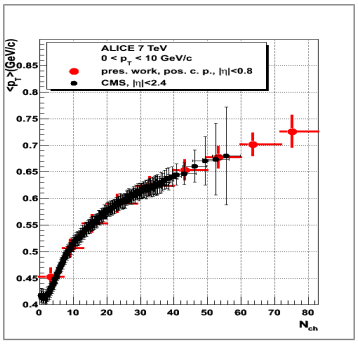

Fig. 4

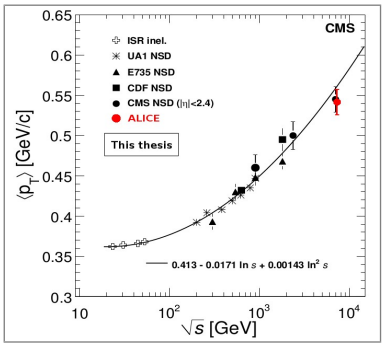

Fig. 5

In Fig. 4, a comparison between the results obtained by us and those obtained in the CMS Collaboration is presented. As can be seen, the agreement is excellent, our data going to higher multiplicities relative to the CMS data. In Fig. 5 the <pT> value without any condition in the charged particle multiplicity is presented by the red symbol. In the error bars limits, our result corresponds to the predicted value using the extrapolation of the results at lower energies and is in perfect agreement with the CMS Collaboration value.

In parallel, the analysis of the positive charged hadrons π+, K+ and protons (p) was done [1] and their pT spectra were obtained. The identification was done using the Bayesian method. The obtained spectra for the eight combined multiplicity ranges and without multiplicity condition (MB) are presented in Fig. 6, upper row.

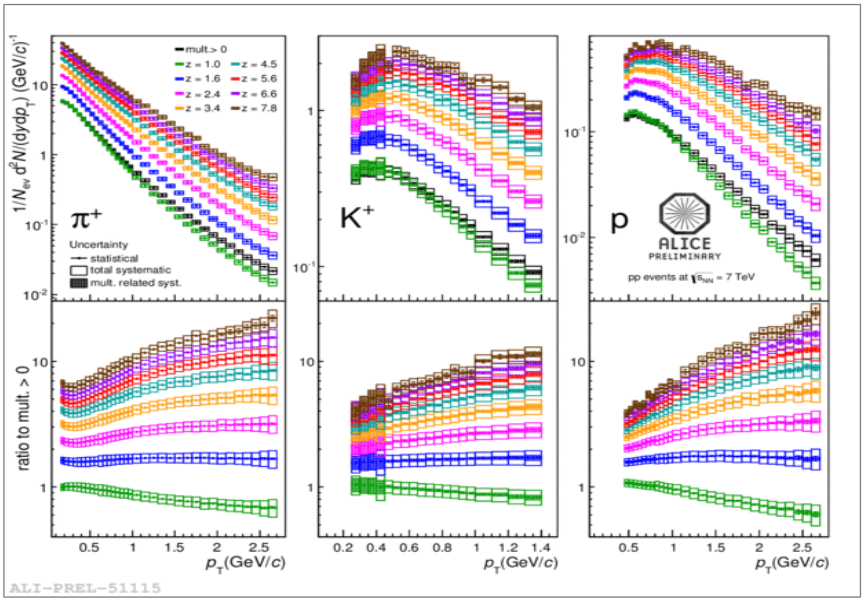

Fig. 6

On the lower row the ratios of spectra for different multiplicity intervals relative to the MB one

are presented. The tendency of the similar ratios corresponding to the charged particles, discussed above, is observed also for identified charged hadrons, the effect increasing with hadron mass from pions to protons. This trend, similar to the one observed in the Pb-Pb collision at the energy of 2.76 TeV, gives a stronger support to the hypothesis of existence of a collective type expansion. Another experimental result which supports this hypothesis can be followed in Fig. 7 where the relative ratios of the yields of the various positive hadron species as a function of p_T are presented on the upper row and their ratios relative to the MB ratio in the lower row.

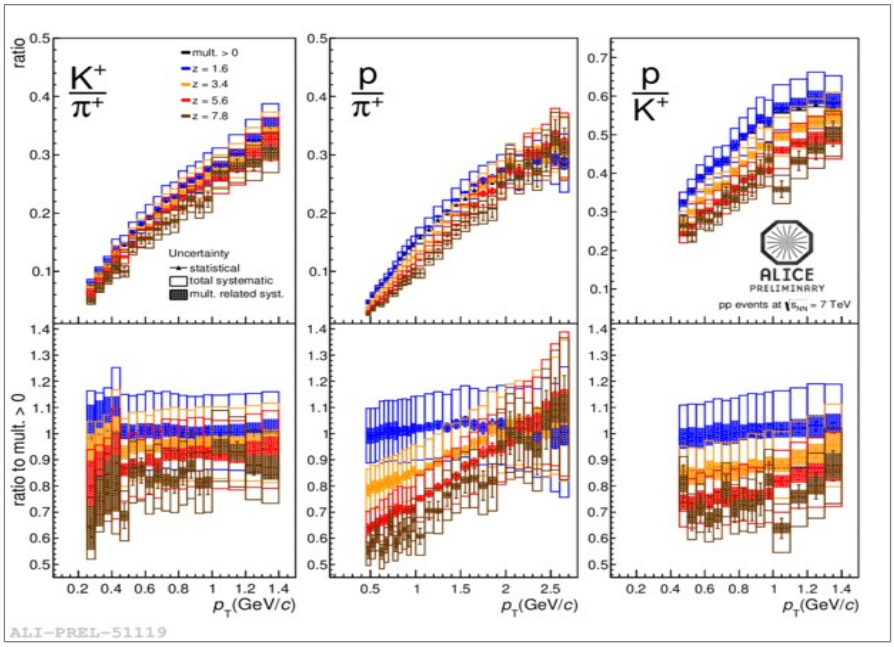

Fig. 7

Similarly to the procedure used for charged particles average transverse momentum values $<P_T>$ for π+, K+ and p were obtained which are presented in Fig. 8. An increase of the average transverse momentum value as a function of multiplicity for all three species can be observed, the increase depending on the particle mass. By representing $<p_T>$ as a function of particle mass for different multiplicity ranges, Fig. 9, an increase of the $<p_{T>}$ slope as a function of mass with increasing of the charged particle multiplicity comes into prominence. This trend clearly shows the existence of a collective type motion on which a statistical type distribution is superimposed.

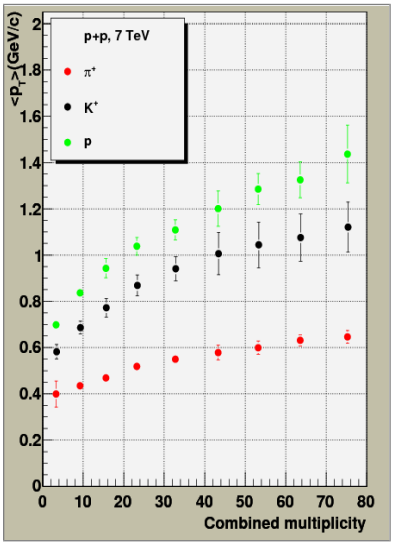

Fig. 8

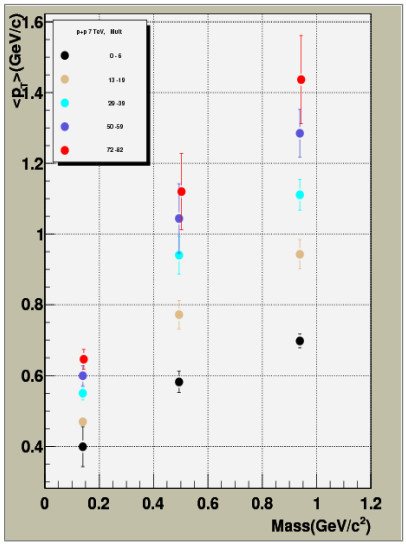

Fig. 9

- Blast wave model fits and comparison with p-Pb and Pb-Pb collisions

The above multiplicity dependent pp data were compared with data obtained in p-Pb and Pb-Pb collisions.
The p_T dependence of p/π for the second and highest multiplicity bins and of $(p + p)/(\pi^+ + \pi^-)$ ratio for p–Pb in 60–80% and 0–5% multiplicity classes and for Pb–Pb at 80–90% and 0–5% centralities [2] are presented in Fig. 10(a) and Fig. 10(b), respectively. The push of protons towards larger p_T values relative to pions with increasing centrality or multiplicity is present for all three systems. Quantitatively, this can be followed in Fig. 10(c) where the ratios of the ratios shown in Fig. 10(a) and Fig. 10(b) are presented. The ratio for pp follows closely the p–Pb trend as a function of p_T.

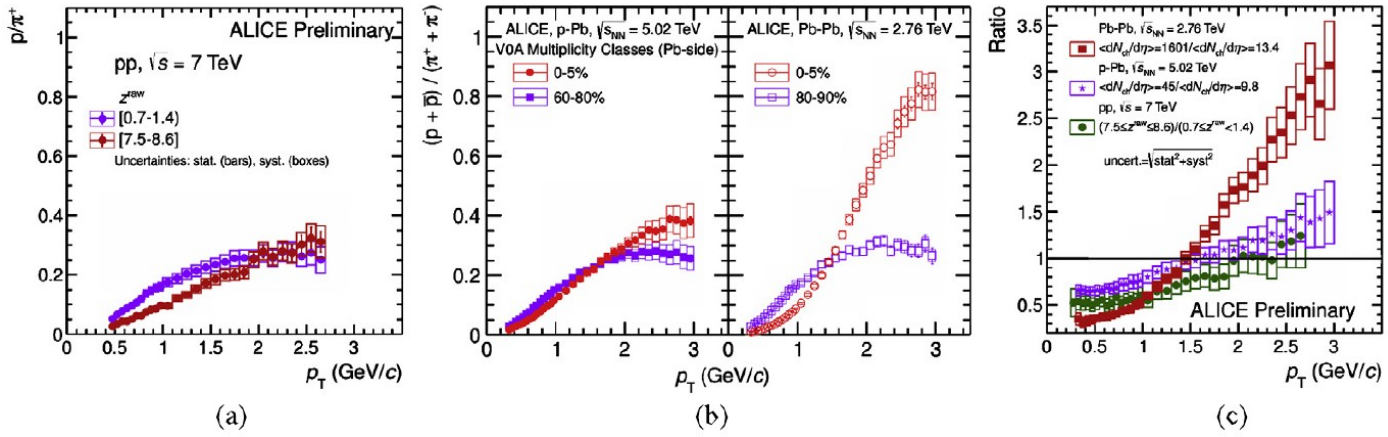

Fig. 10

Based on these similarities, information on collective type dynamics from the fits of experimental transverse momentum spectra using expressions inspired by hydrodynamical models [3] was obtained. The average transverse expansion velocity and kinetic freeze-out temperature were obtained as parameters of the following expression used for the fit:

$$E\frac{d^3N}{dp^3} \sim f(p_t) = \int_0^R m_T K_1(m_T cosh\rho/T_{fo}) I_0(p_T sinh\rho/T_{fo}) r dr$$

where:

$$m_T = \sqrt{m^2 + p_T^2};\ \beta_r(r) = \beta_s(\tfrac{r}{R})^n;\ \rho = tanh^{-1}\beta_r$$

The result of these fits done simultaneously on π + , K+ and p spectra, in terms of T_{kin} - $< \beta_T >$ correlation as a function of charged particle multiplicity and comparison with the results obtained for Pb-Pb and p-Pb as a function of centrality and multiplicity classes, respectively, are presented in Fig.11(a) [1]. One could conclude that for pp collisions at 7 TeV, the T_{kin} - $< \beta_T >$ correlation as a function of charged particle multiplicity has a trend rather similar with the one observed in heavy ion collisions, i.e. the freeze-out kinetic temperature decreases and the average transverse expansion velocity increases with charged particle multiplicity (pp) or increasing centrality (A-A). However, there is a quantitative difference between pp and A-A collisions, i.e. T_{kin} is systematically lower and $< \beta_T >$ systematically larger than the pp values, the difference increasing towards higher centralities. Within the error bars, the results for p-Pb at 5.02 TeV are the same with the ones evidenced in pp. Such a correlation is not reproduced by PYTHIA for the pp case. Including the color reconnection mechanism [4] it seems that the model starts to show a similar trend but with values of T_{kin} about 40 MeV lower. On Fig. 11(b) a similar plot [5] is shown, including all energies measured at RHIC [5] and Pb-Pb at 2.76 TeV at LHC [6].

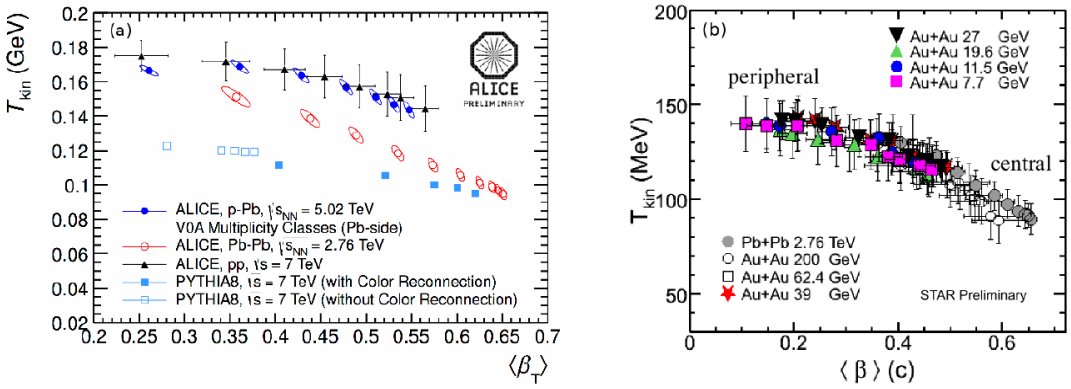

Fig. 11

Another aspect worth to be mentioned is the correlation between the expansion profile (n) and $< \beta_T >$. This correlation is presented in Fig. 12(a) [1]. It is clearly seen that all three systems follow exactly the same correlation. Towards the highest multiplicity in the pp case, the expansion velocity becomes linear as a function of position within the fireball. The n - $1/T_{kin}$ correlation (Fig. 12(b)) shows that the PYTHIA prediction is completely different than the experimental one.

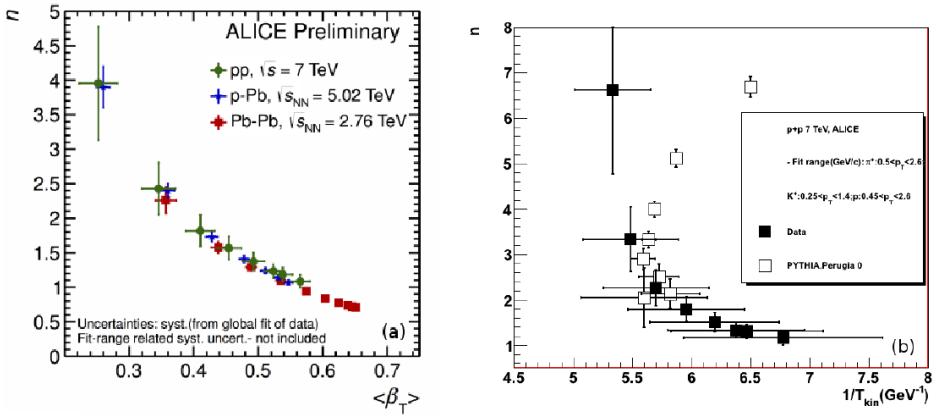

Fig. 12

- *<p_T> and yields*

As mentioned above further studies regarding the multiplicity selector dependence have been started in parallel. Similar to heavier systems, the studies based on the forward detector V0M amplitude selection were triggered by the necessity to minimize the autocorrelation effects, if they manifest, and compare systems on the same basis. Charged particle and identified hadron spectra have been obtained in different percentiles (specified in the plots) and in Figs. 13, 14, 15 below are shown the ones for pions, kaons and protons. For this V0M selector the range in p_T for PID data analysis has been significantly enlarged by combining several analyses on different transverse momentum ranges. The data have been presented at Quark Matter 2015 Conference.

Starting from these large transverse momentum range spectra the average transverse momentum and yields have been extracted using different fit functions. The fit quality for different fit functions is shown in Figs. 16 and 17. The functions are named 1 to 3 from left to right in Fig. 16 and 4 and 5 from left to right in Fig. 17.

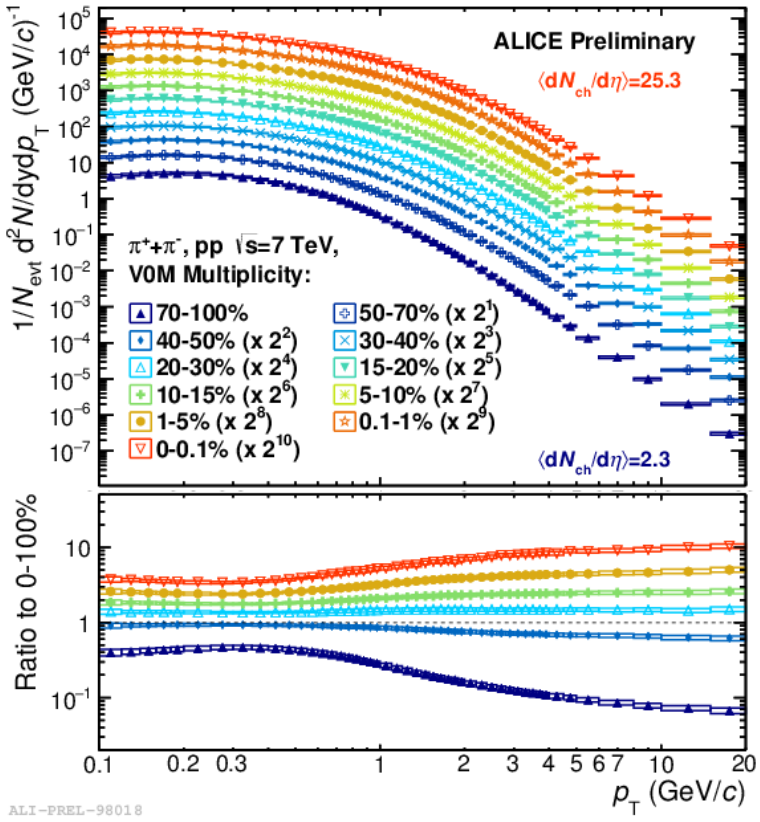
ALICE Preliminary
⟨dN_ch/dη⟩=25.3
π⁺+π⁻, pp √s=7 TeV,
V0M Multiplicity:
70-100%
40-50% (x 2²)
20-30% (x 2⁴)
10-15% (x 2⁶)
1-5% (x 2⁸)
0-0.1% (x 2¹⁰)
50-70% (x 2¹)
30-40% (x 2³)
15-20% (x 2⁵)
5-10% (x 2⁷)
0.1-1% (x 2⁹)
⟨dN_ch/dη⟩=2.3
1/N_evt d²N/dydp_T (GeV/c)⁻¹
Ratio to 0-100%
p_T (GeV/c)
ALI-PREL-98018

Fig. 13

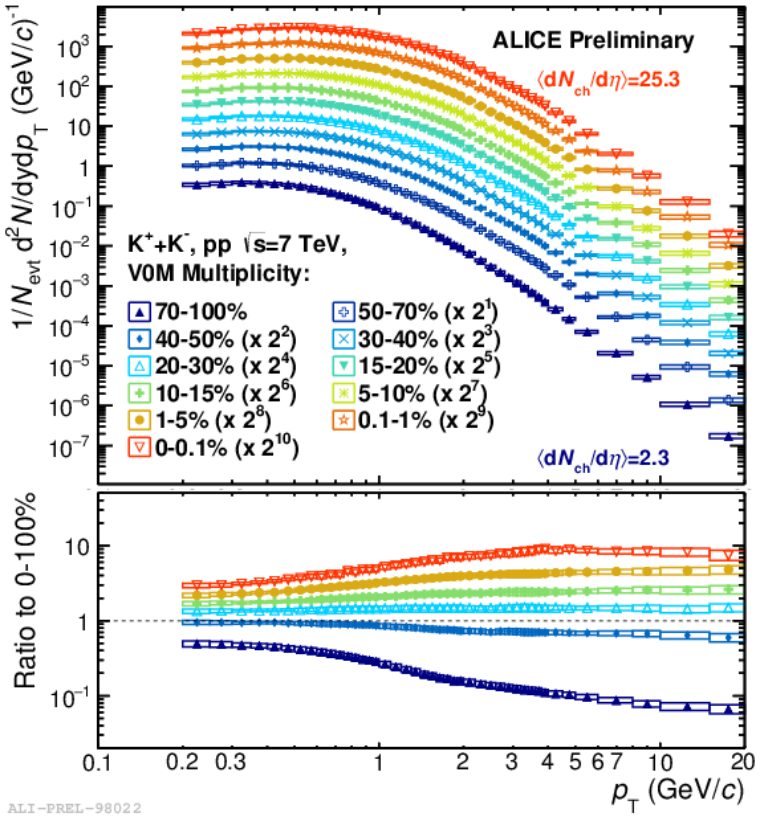
ALICE Preliminary
⟨dN_ch/dη⟩=25.3
K⁺+K⁻, pp √s=7 TeV,
V0M Multiplicity:
70-100%
40-50% (x 2²)
20-30% (x 2⁴)
10-15% (x 2⁶)
1-5% (x 2⁸)
0-0.1% (x 2¹⁰)
50-70% (x 2¹)
30-40% (x 2³)
15-20% (x 2⁵)
5-10% (x 2⁷)
0.1-1% (x 2⁹)
⟨dN_ch/dη⟩=2.3
1/N_evt d²N/dydp_T (GeV/c)⁻¹
Ratio to 0-100%
p_T (GeV/c)
ALI-PREL-98022

Fig. 14

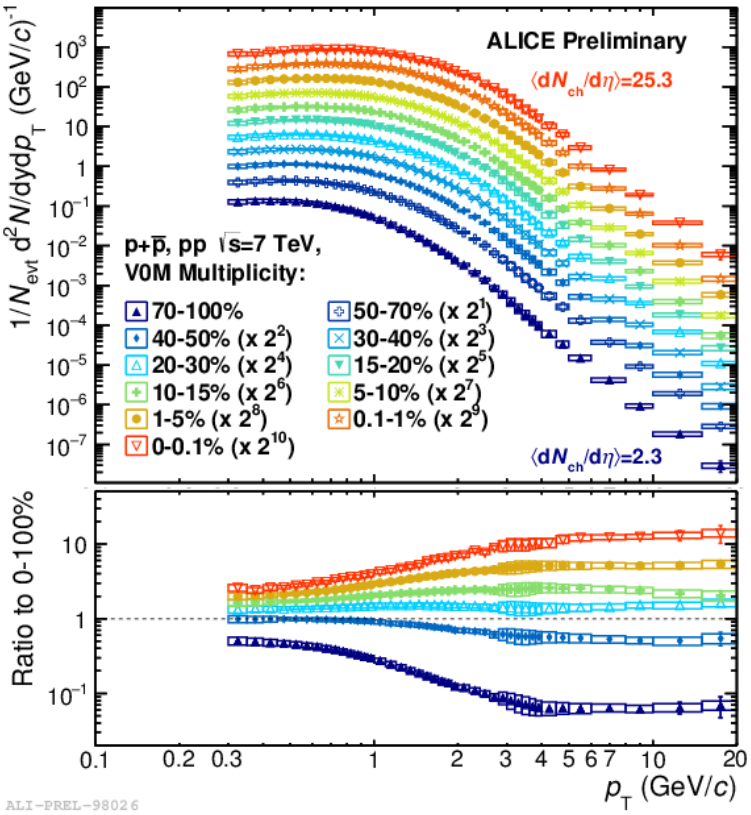
ALICE Preliminary
⟨dN_ch/dη⟩=25.3
⟨dN_ch/dη⟩=2.3
p+p̄, pp √s=7 TeV,
V0M Multiplicity:
70-100%
40-50% (x 2^2)
20-30% (x 2^4)
10-15% (x 2^6)
1-5% (x 2^8)
0-0.1% (x 2^10)
50-70% (x 2^1)
30-40% (x 2^3)
15-20% (x 2^5)
5-10% (x 2^7)
0.1-1% (x 2^9)
1/N_evt d^2N/dydp_T (GeV/c)^-1
Ratio to 0-100%
p_T (GeV/c)
ALI-PREL-98026

Fig. 15

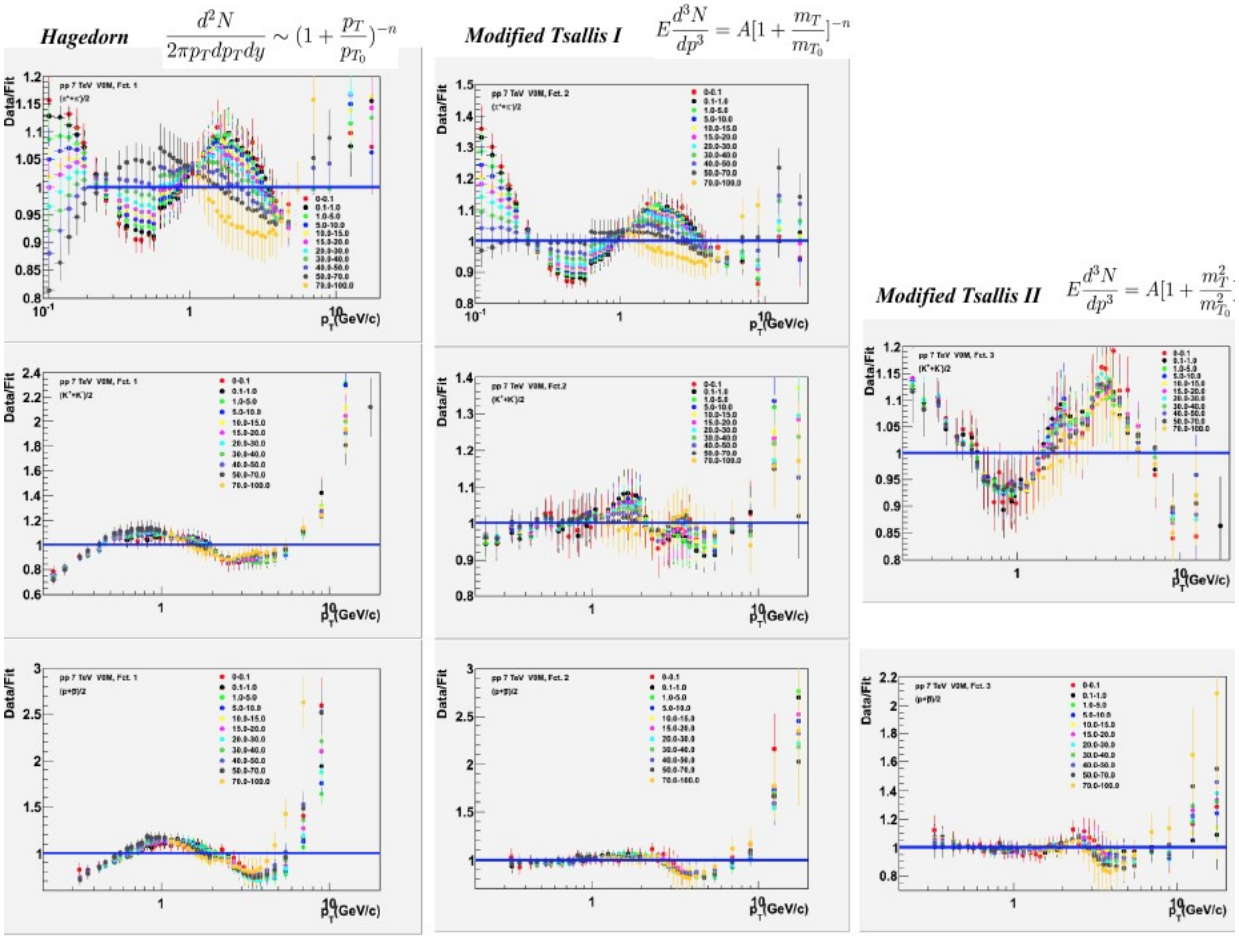
Hagedorn
$\frac{d^2N}{2\pi p_T dp_T dy} \sim (1+\frac{p_T}{p_{T_0}})^{-n}$
Modified Tsallis I
$E\frac{d^3N}{dp^3} = A[1+\frac{m_T}{m_{T_0}}]^{-n}$
Modified Tsallis II
$E\frac{d^3N}{dp^3} = A[1+\frac{m_T^2}{m_{T_0}^2}]$
Data/Fit
p_T (GeV/c)

Fig. 16

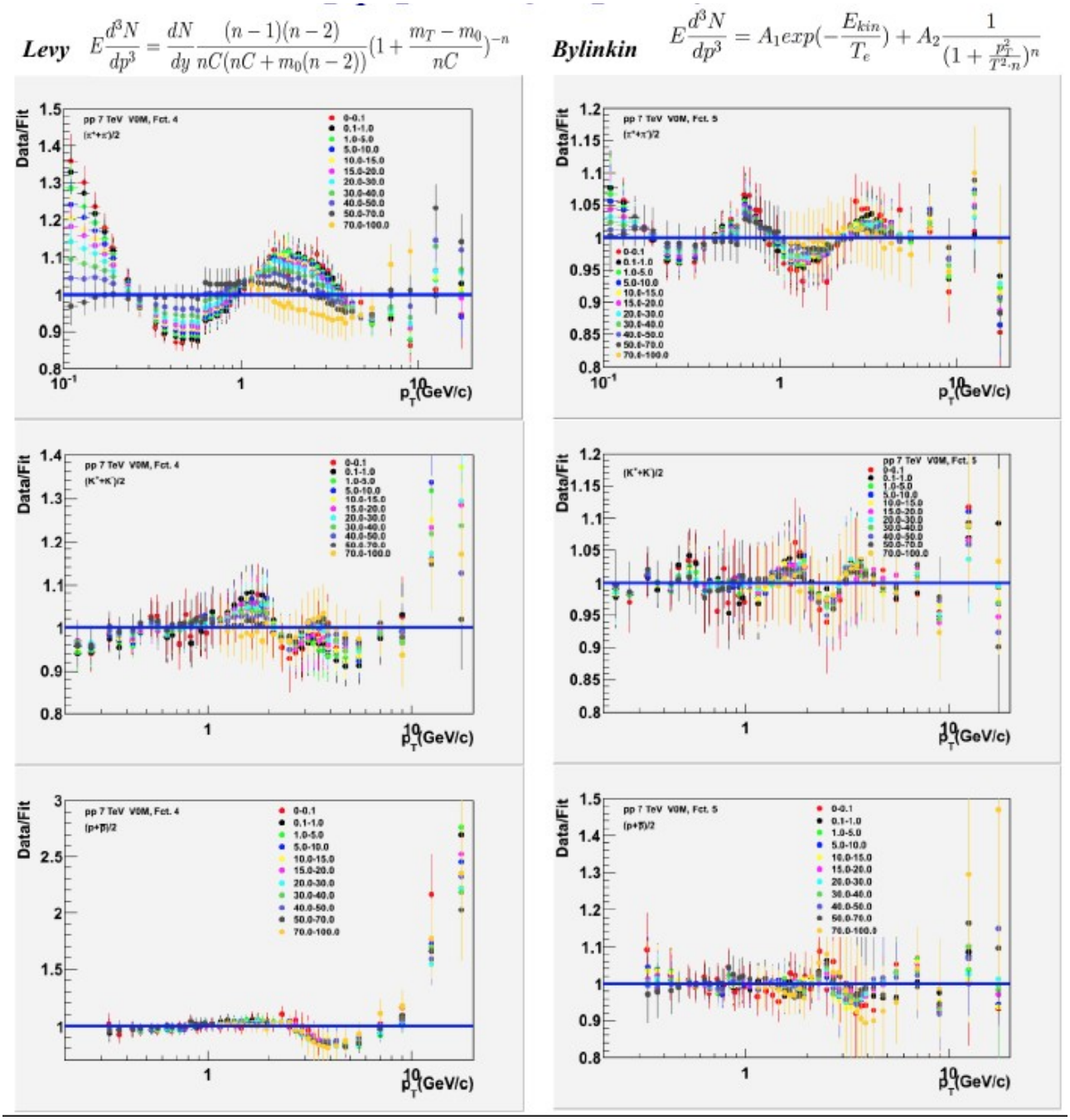

Fig. 17

The fit quality for function 5 (Bylinkin) is the best one (in the limit of 5% variation of the data to fit ratio).

The results for $\langle p_T \rangle$ and yield ratios are shown in Figs. 18 and 19 for the different fit functions.

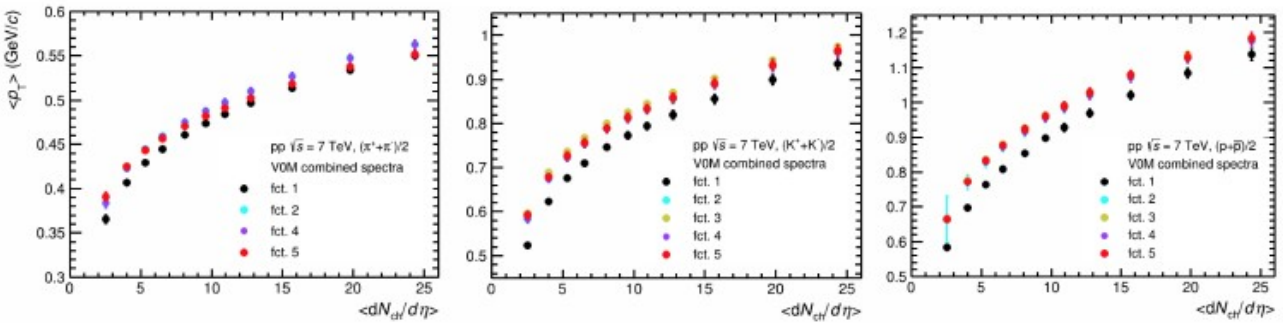

Fig. 18

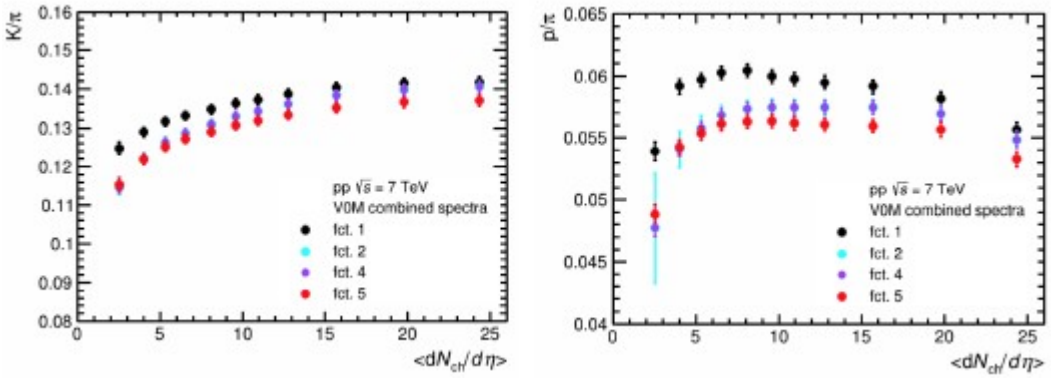

Fig. 19

The difference between the best fit function results and the others can be used to esimate the systematic error due to the fit.

b. Event shape studies

The hadronic final states formed in high energy collisions can manifest different topologies depending on the underlying processes. The topology of each event can be characterized by several event shape variables built using the detected particles. By definition, the event shape observables are designed to measure the energy flow in the collision. They are constructed using both the orientation and the magnitude of each particle momentum. Several event shape observables - ESO - have been used for more than forty years in high energy physics. Originally, these observables were used in jet studies to evidence parton hard scatterings that translate into hadronic jets. The study of jets is a central part of the perturbative QCD studies that extract the properties of quarks and gluons from the hadron distribution in the final event. Using a different approach, in this analysis, event shape observables are used to identify events with random particle distributions. A uniform particle distribution is specific to a non-jetty event. Such isotropic events could reveal properties of the matter created in the collision in the soft region of the spectrum, region described phenomenologically. This approach raises some questions on the event selection performance of the event shape observables. Can events with jets be labeled as uniform by using the event shapes? Is it possible to use the same observables that are used to select jetty events to clean the data sample? Are the selected events in any way biased? Is there a spectrum that randomly distributed in azimuth is not biased by the event shape selection?
The event shape observables studied are:
- Directivity – D -measures the normalized momentum deviation from 0 in the positive or negative η ranges [7,8].
- Thrust – T – [9,10] is defined as the normalized maximum value of the momentum projection on an arbitrary axis, summed over all particles in the event.
- Sphericity – S - was introduced in [11] and it measures how close to being spherical the particle distribution in the event is. The spherical shape will be replaced by a circular one when the particles are projected in the transverse plane.

- Recoil – R - measures how well the momentum conservation is reconstructed in the event [12].
- Fox-Wolfram moments – FWM – were introduced by G.C. Fox and S. Wolfram in [13].

- *Charged particles [14]*

Particles reconstructed in analyzed events do not always originate in the primary vertex. The most probable sources of contamination are particle decays and secondaries produced in the particle interaction with the material present in the experiment. Also, some particles will not be detected due to the limited acceptance and efficiency or the interaction with the material. Both effects can be evaluated using Monte Carlo simulations once the detector response and the material distribution in the experiment are known. Therefore, the efficiency dependence on the event shape cuts was also studied for all the event shape selectors presented above.

For all the multiplicity bins the event shape cuts were applied. The transverse momentum spectra for event shape cuts in all the combined multiplicity bins are presented. The efficiency correction was done bin wise. The feed-down correction used was the one from minimum bias, the same as for the minimum bias multiplicity spectra. For the minimum bias multiplicity bins, the results for sphericity (S), directivity (D), thrust (T) and Fox-Wolfram cuts are plotted in Figures 20,21,22,23, respectively. The multiplicity bins are displayed as follows: the first three bins are plotted in order on the first row and the last three bin on the second row. The Fox-Wolfram moments cuts correspond to isotropic and non-isotropic events. All the spectra are normalized to the number of events analyzed in the corresponding class. For all the event shape cuts, the spectra for "non-isotropic" events have long tails. The events labeled as "isotropic" have a "softer" shape.

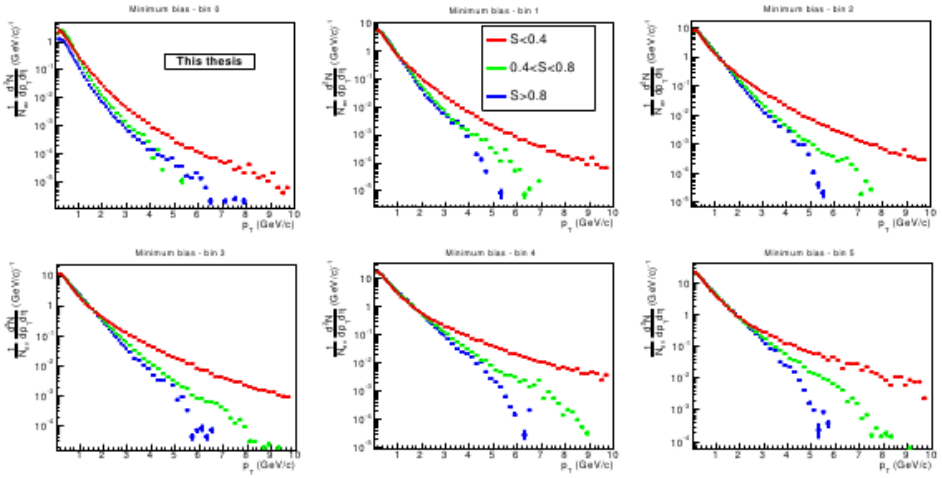

Fig. 20

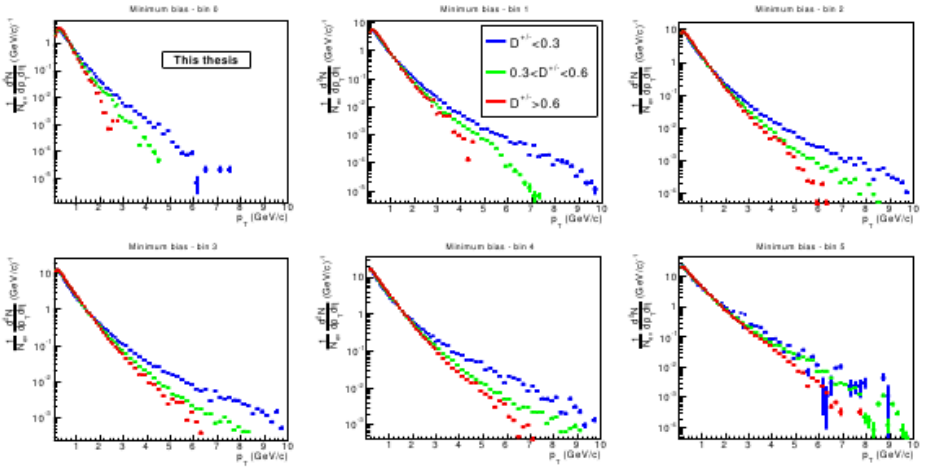

Fig. 21

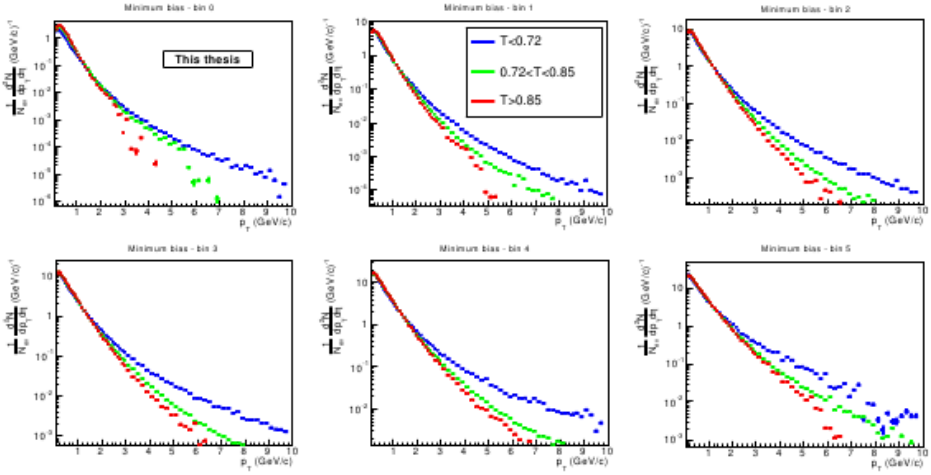

Fig. 22

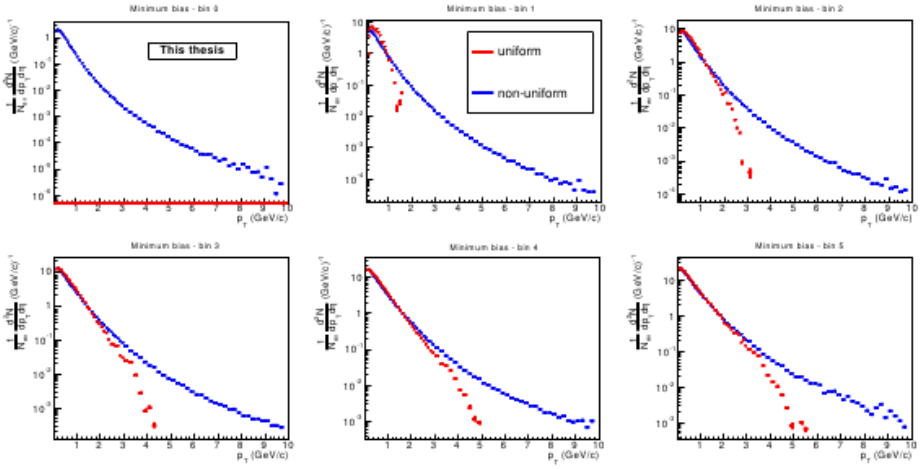

Fig. 23

The spectra for events close to azimuthal isotropy, selected with the sphericity (Fig. 24 left), thrust (Fig. 24 right), directivity (Fig. 25 left)and Fox-Wolfram moments (Fig. 25 right) are plotted. The slope of the transverse momentum distributions for the events selected in this way, is changing with the multiplicity. The power law tails observed in the p_T spectra for different

multiplicity bins are drastically reduced in Figures 24 and 25 where nearly azimuthal isotropic events were selected.

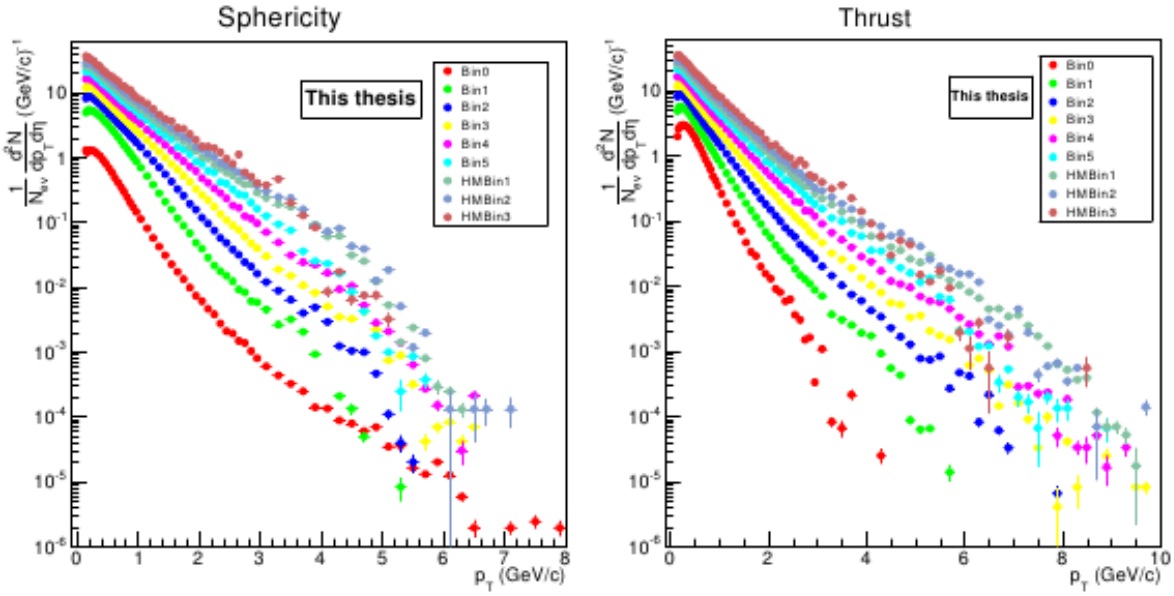

Fig. 24

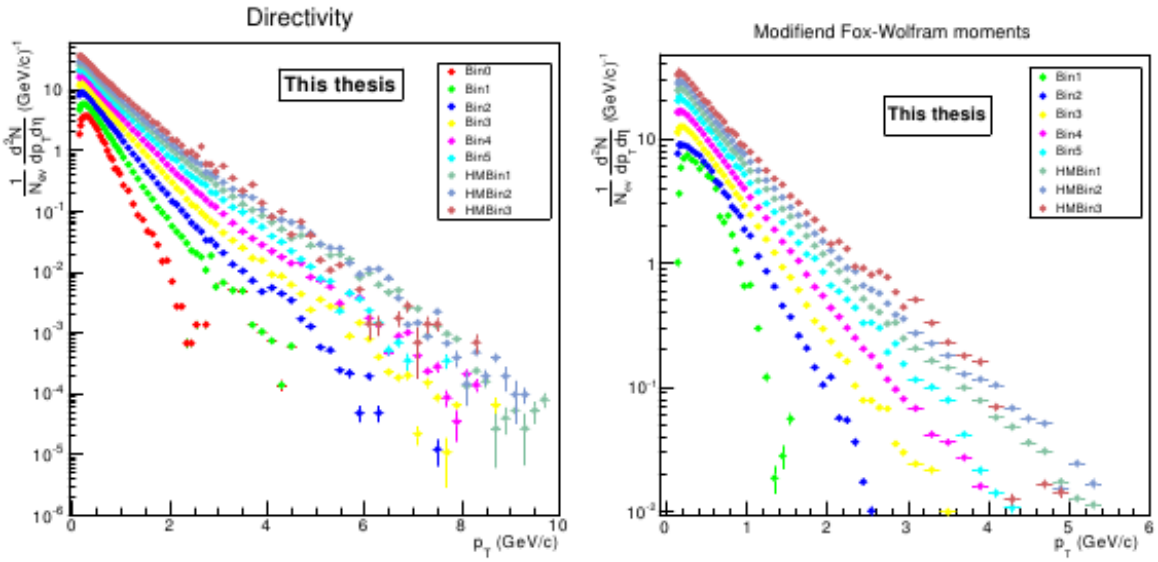

Fig. 25

- *Identified charged hadrons [15,16]*

Events close to azimuthal isotropy are of a special interest for this analysis. In order to estimate the degree of azimuthal isotropy the global observable directivity was used. This observable is defined as:

$$D^{\pm} = \frac{\left|\sum_i \vec{p}_t^{\,i}\right|}{\sum_i \left|\vec{p}_t^{\,i}\right|}\Big|_{\eta^{pos/neg}>}$$

As it can be seen from the formula, the events with a high azimuthal isotropy will have a low directivity. For events dominated by jets the directivity increases towards 1.

The two dimensional directivity (computed as the mean of D^+ and D^-) versus multiplicity representation is shown in Fig. 26.

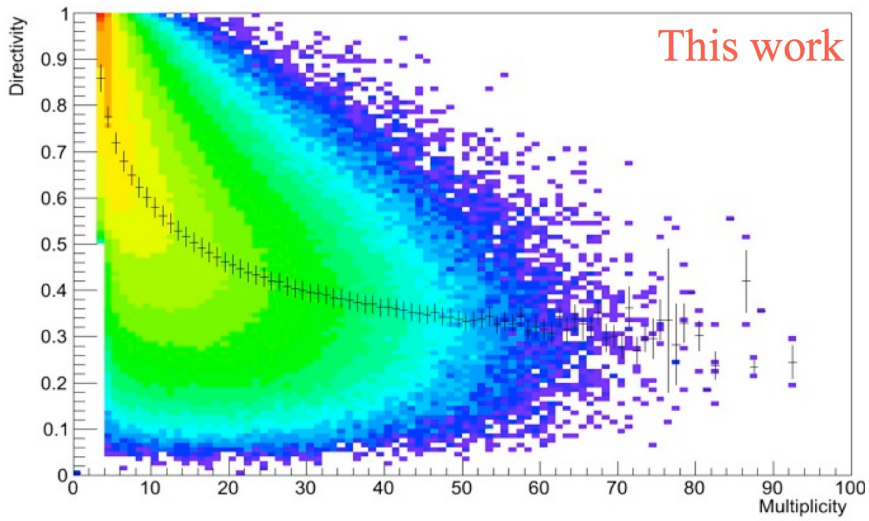

Fig. 26

$d^2N/\Delta\varphi\Delta\eta$ two dimensional representations for minimum bias and multiplicity >30 & directivity <0.3, where $\Delta\varphi$ and $\Delta\eta$ represent the difference in pseudorapidity and azimuthal angle between a given identified charged hadron and the leading particle in the respective event, used in order to evaluate the performance of the event shape selection, are shown in Fig. 27 (minimum bias case) and Fig. 28 (M>30 & D<0.3 case) .

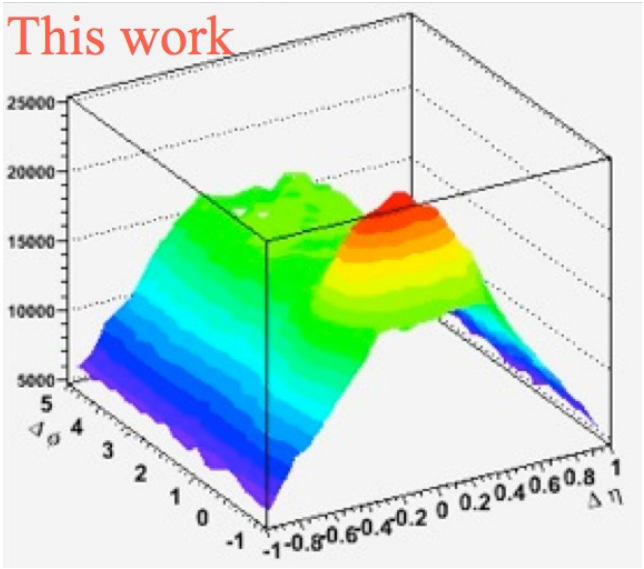

Fig. 27

Even without extracting the background correlation one could observe, comparing the two distributions, that high multiplicity and low directivity cut removes the jet-like correlation observed in the minimum bias case [16].

In the case of the selections using the events multiplicity based on the combined multiplicity estimator, there is no dependence of the corrections as a function of multiplicity. When on top of the multiplicity selection an extra cut using the event directivity is applied this is no longer the case. For the low multiplicity bins the corrections show a strong variation with the directivity of the considered events. However, as the multiplicity increases this dependence reduces very fast.

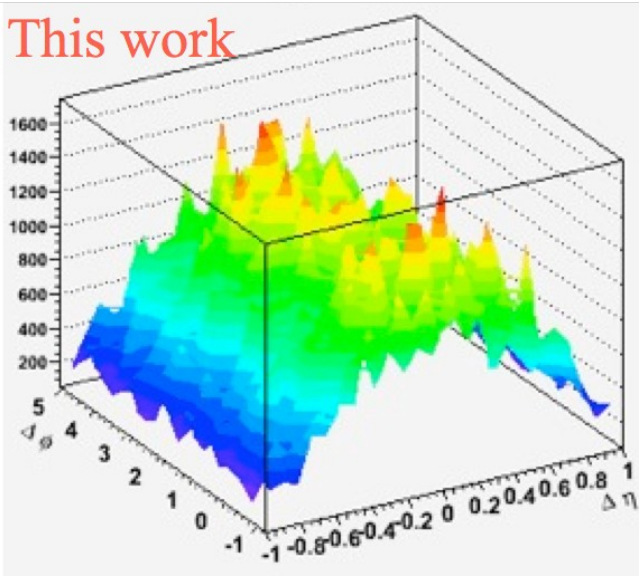

Fig. 28

For a combined multiplicity above 40 this variation is below 3%. Consequently, as in the case of the spectra in multiplicity bins, the MB determined corrections were used also for the spectra in directivity bins, only for events with multiplicity above 40. The mentioned 3% variation for the tracking, matching, PID efficiency and percentage of misidentified particles was included in the systematic errors. For this analysis three directivity ranges were established: directivity lower then 0.3, 0.3 to 0.6 and 0.6 to 0.9. In order to consider an event to be in one of the above mentioned directivity classes both D^+ and D^- have to fulfill simultaneously the imposed condition. A visual representation of the selected events in terms of mean directivity and combined multiplicity is shown in Fig. 29, where only events for which the simultaneous D^+ and D^- condition was fulfilled. This procedure selects samples with high purity but it decreases considerably the available statistics. The studies done with the simultaneously imposed condition have shown that at the largest multiplicity bins a change in the shape of the spectra is present for the low directivity case. Unfortunately it is difficult to further exploit the spectra obtained in such low statistics conditions. Thus we choose to study the parameter variations of the fit on the directivity selected spectra by constraining them only on D^+.

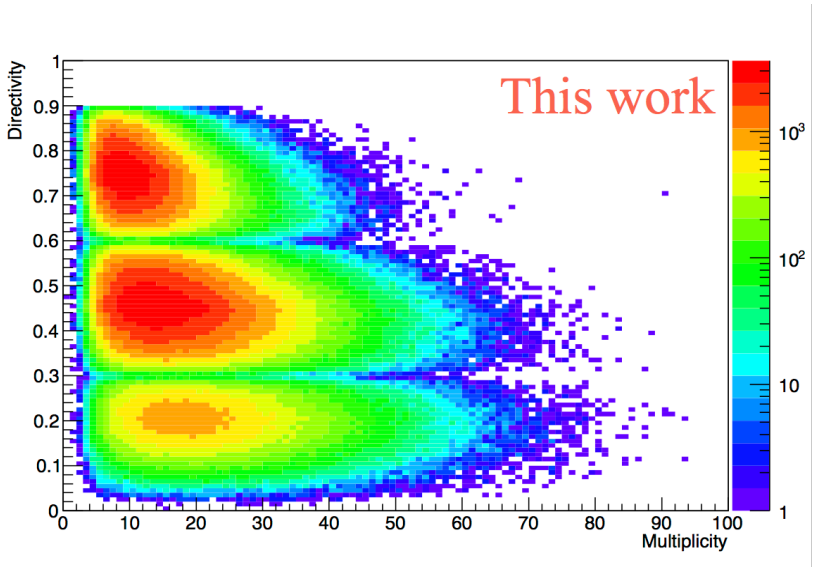

Fig. 29

The fully corrected p_T spectra were obtained by selecting events defined based on their directivity computed for $\eta > 0$, in addition to selection of events based on their multiplicity, which was used until now.

For each multiplicity class (1-6, 7-12, 13-19, 20-28, 29-39, 40-49) three directivity based event classes were defined (0 - 0.3, 0.3 - 0.6 and 0.6 - 1.0). As before, the multiplicity was estimated by summing the global tracks and complementary Inner Tracking System (ITS) standalone tracks and Silicon Pixel Detector (SPD) tracklets in $|\eta|<0.8$.

This study was performed using our local computing farm (NAF) to analyze approximatively $1.4 \cdot 10^7$ events measured by the ALICE experiment at the LHC during the 2010 data taking period. The selections used for the tracks considered in the analysis and the particle identification procedure were the same as the ones used for the previously reported results, which were obtained using only multiplicity classes.

A similar number of Monte-Carlo simulated events, based on the PYTHIA event generator, which were produced using the specific detector state of the corresponding data taking period, were used in order to determine the necessary corrections.

In the case of the spectra defined only by selections in multiplicity, the corrections showed no variation for the different event classes. This has allowed us to use only one set of corrections, which were determined using all the available Monte-Carlo generated data without applying any event selections. However, when one considers also the shape of the event, in addition to its multiplicity, when defining the event classes, significant differences in the determined corrections are obtained. Therefore, for this study, we have obtained the corrections for each multiplicity-directivity event class and we have applied it to the corresponding raw data.

The results, for the above specified selections in multiplicity and directivity are shown in Figure 1, for pions, kaons and protons. The intermediate directivity class (0.3 - 0.6) is not plotted. For completeness the spectra obtained without any selection in multiplicity (black symbols) and the spectra obtained without any selection in directivity (full squares) are also included in Fig. 30.

In the bottom row the ratios of the spectra obtained with selections in directivity to the spectrum in the corresponding multiplicity class are plotted.

The open crosses in the bottom row are included in order to provide a crosscheck by comparing the already preliminary spectra, obtained using only the selection in multiplicity, with the new results. Taking into consideration that the lowest multiplicity bin (1-6) is not a preliminary result for any specie and the fact that the preliminary kaon spectra has to be considered only up to 1.4 GeV, this crosscheck is rather satisfactory.

A simultaneous fit of the pT spectra of π±, K± and p, pbar was done using the well known Boltzmann-Gibbs Blast Wave expression inspired by hydrodynamical models, mentioned before [3]:

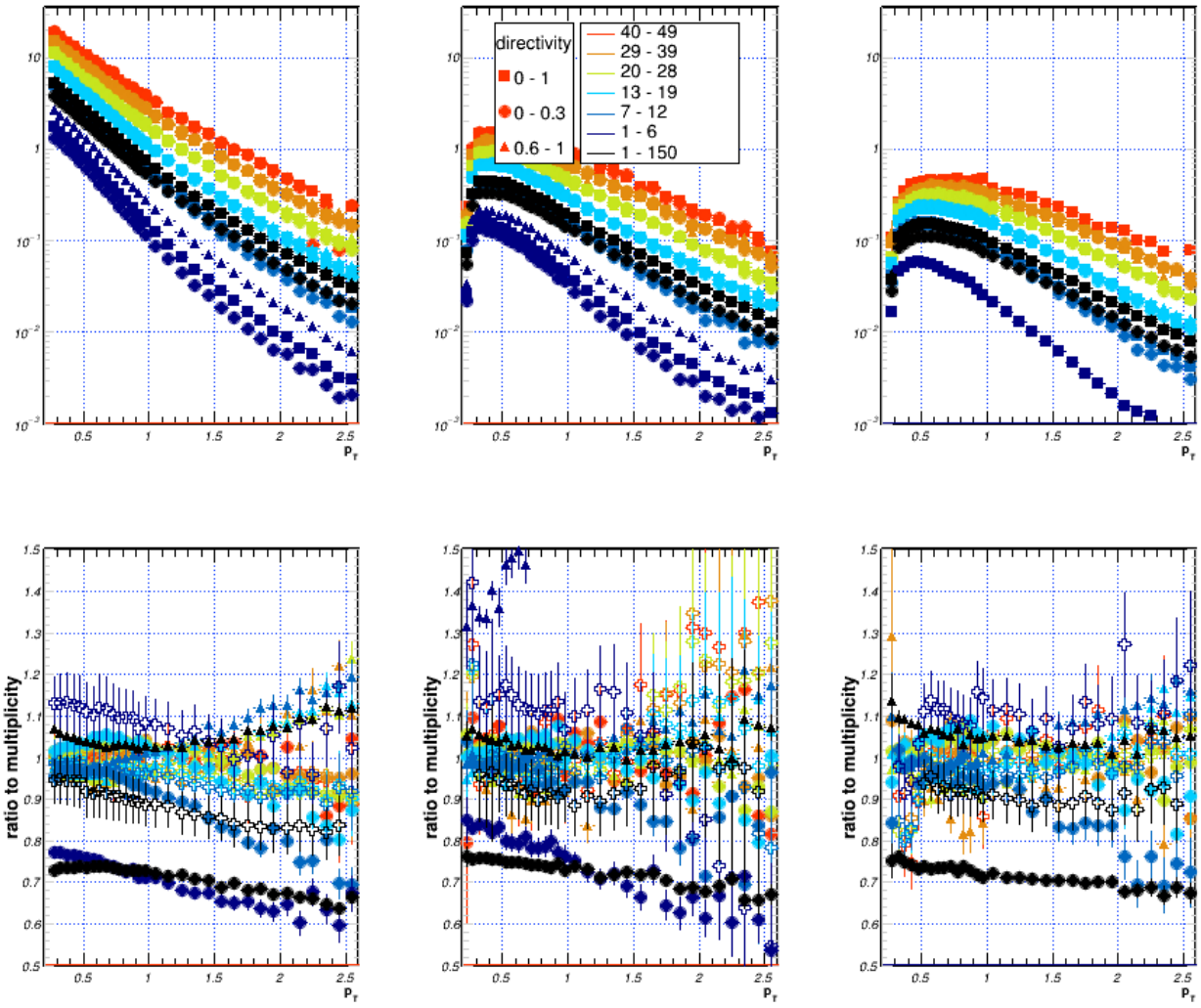

Fig. 30

The fit was done on spectra without directivity constraint, directivity between 0-0.3 and 0.3-0.6 respectively. Two ranges of fit were used, namely a restricted one corresponding to the maximum range in p_T in Pb-Pb spectra where the suppression is not present (established on the model independent representations we have done for comparing the three systems measured at LHC: pp at 7 TeV, p-Pb at 5.02 TeV and Pb-Pb at 2.76 Tev). The larger fit range with K and p up to 3 GeV in p_T was used in order to see the sensitivity to the fit range. The lower p_T limits were established for pions to reduce the contribution of resonance decays at low p_T and for kaons and protons by the experimental threshold.

In Figures 31 and 32 are represented the T_{fo}-$<\beta_T>$ and n-$<\beta_T>$ parameter correlations for all selections in multiplicity and directivity. Although for the low directivity cut the average transverse expansion velocity is a bit higher than in the other cases and the n parameter a bit lower, in the limit of the errors of fit parameters there is no significant difference for the three

cases. In the quality fit plots for all species with no directivity cut, 0.3-0.6 cut and 0.0-0.3 respectively, and from the χ^2 value one can say that the fit quality improves for cuts in directivity and with increasing multiplicity, being slightly better for the lower directivity cut. Increasing the statistics on higher multiplicity bins by including other pp data productions and applying other event shape selectors have to be considered in the future. The difficulty of these studies consists in applying the efficiency correction which might need a more elaborate procedure of calculation (simultaneous multidimensional unfolding) than the one to one bin correction.

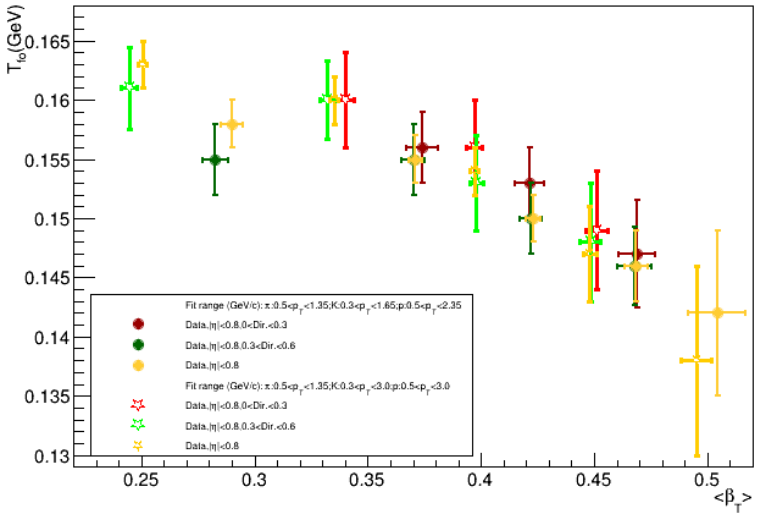

Fig. 31

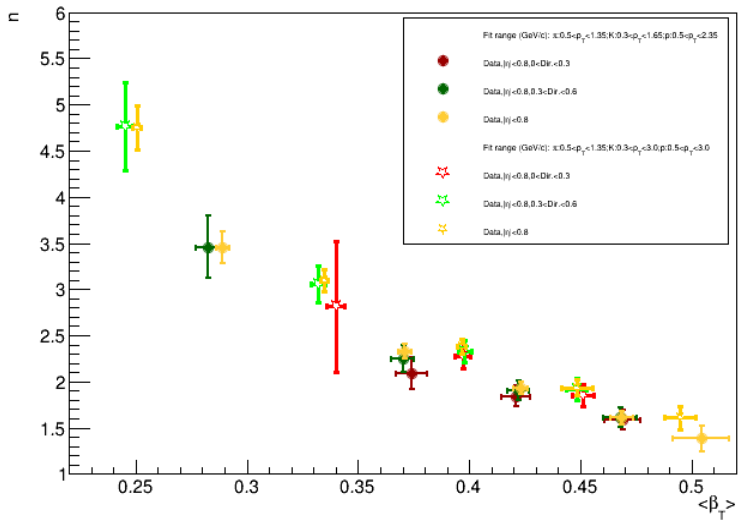

Fig. 32

Conclusions

The possibility to select highly isotropic events in pp collisions at 7 TeV has been studied on the experimental data. The shapes of the obtained spectra in different multiplicity & event shape selections clearly depend on the selection variable and its value. By combining several detectors

extended spectra in the average transverse momentum have been obtained for different multiplicity estimators for charged particles and identified hadrons. Based on these, several fit formulas of the spectra can be used in order to obtain the average transverse momentum and yield ratios. Similarities with the p-Pb and Pb-Pb data have been seen in the frame of a Blast Wave phenomenological model. This analysis is quite robust now and is subject to an extended paper in whose preparation our group is also involved. More statistics and further checks on the efficiency corrections are needed in order to draw firm conclusions on the behaviour of the similar observables selected also with different event shape variables.

- ***Glauber model predictions in comparing pp, p-Pb and Pb-Pb systems***

One of the observables sensitive to the production mechanism of particles and the partonic structure of the colliding objects is the charged particle density and its dependence on the collision geometry. Detailed information on the centrality dependence of the charged particle density at mid-rapidity in A-A collisions is available starting from the AGS energies, to SPS and up to RHIC. At SPS and AGS energies, in the systematic errors limit, the normalized charged particle density dNch/dη/(0.5Npart) is quite constant as a function of centrality, namely Npart estimated on the basis of Glauber model. Although the dependence of the dNch/dη/(0.5Npart) shape on Npart is fairly similar at 130 and 200 GeV, a slight increase of the charged particle density can be observed from the peripheral to the central collisions. This behavior is enhanced at the LHC energy of 2.76 TeV where the published data by ALICE, ATLAS and CMS are in remarkable agreement. As it is expected and confirmed by the Monte Carlo Glauber model, in very peripheral collisions where the two diffused zones of the two colliding nuclei are overlapping, preponderently binary collisions take place and the normalized charged particle density should have the same value as the charged particle density in inelastic nucleon-nucleon collisions. Based on the measurements at ISR, RHIC and LHC for pp collisions the scaling factors (dNch/dη)pp 2.76 TeV/(dNch/dη)pp 0.2 TeV and
(dNch/dη)pp 2.76 TeV/(dNch/dη)pp 0.0196 TeVcan be obtained. Based on the Monte Carlo Glauber model the scaling factors in terms of the ratios of the average number of collisions suffered by the nucleons involved in interaction were estimated: <Ncoll2.76TeV>/<Ncoll0.2 TeV> and <Ncoll2.76TeV>/<Ncoll0.0196 TeV> as a function of Npart. By multiplying the normalized charged particle densities at 19.6 and 200 GeV, with the factors described above, values comparable with the results at 2.76 TeV are obtained (Fig. 33).
In conclusion, a scaling with energy of the centrality dependence of the charged particle density at mid-rapidity, based on the ratio between the charged particle density in inelastic pp collisions and the average number of collisions suffered by the struck nucleons at a given centrality at the corresponding energies, is shown to be valid in the limit of experimental errors.

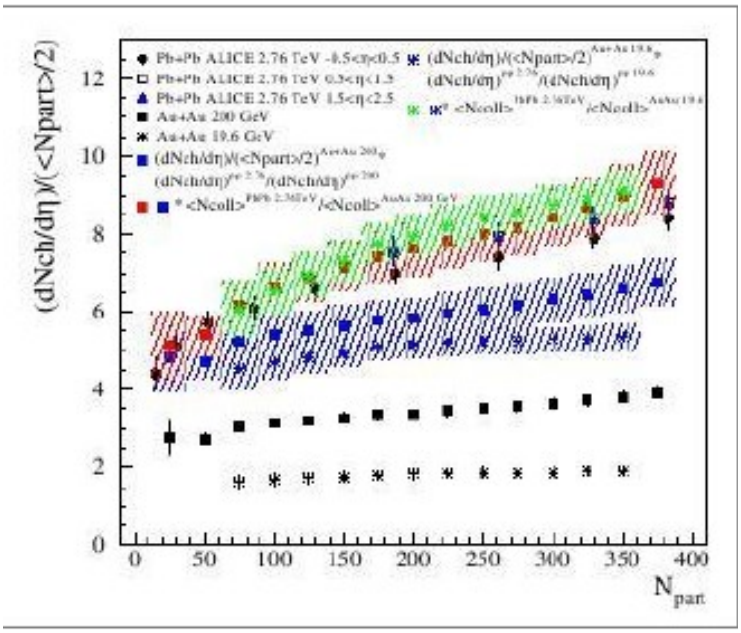

Fig. 33

Estimations based on the Glauber model for the average distances between the centroids of nucleons which participate to the Pb-Pb interaction at 2.76 TeV energy and p-Pb at 5.02 TeV energy were done and compared with the impact parameter in the pp collision at 7 TeV energy using the charged particle multiplicity distribution and various parameterizations of the hadronic matter distribution in the proton, essential in understanding the resemblances and differences in the behavior of various experimental observables in Pb-Pb, p-Pb and pp interactions at the LHC energies. The results are presented in Fig. 34.

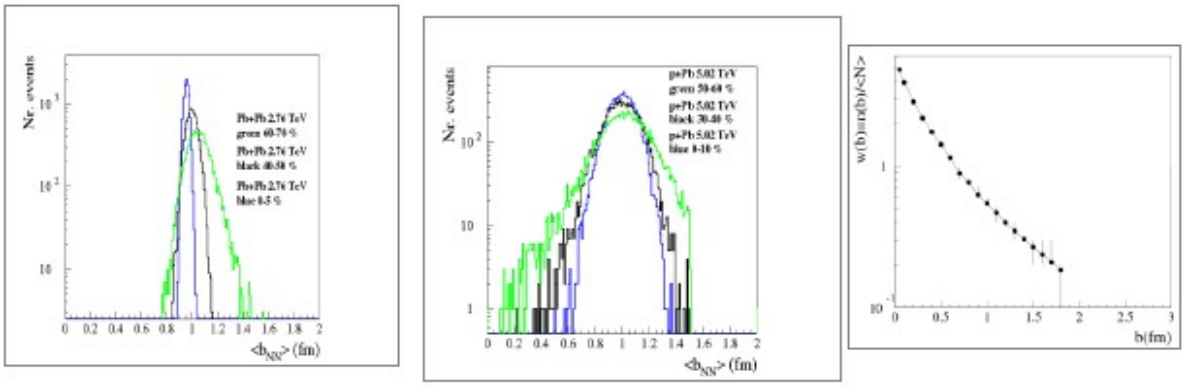

Fig. 34

- ***Comparison of the experimental data with more elaborate phenomenological models***

1. *The HIJING model*

The Large Hadron Collider (LHC) experiments are designed to measure hadronic, leptonic and photonic probes in a large acceptance and at extreme interaction rates and aim at a systematic investigation of Pb+Pb, p+Pb and p+p collisions in terms of collisions energy (from $\sqrt{s_{NN}}$ = 0.9 TeV up to $\sqrt{s_{NN}}$ = 13 TeV) and collision system size, with high precision and statistics.

Event generators like HIJING/BBbar v2.0 determine multiplicities from their models of soft particle production followed by fragmentation and hadronization. Theoretical predictions of particle production in high energy p+p, p+Pb and Pb +Pb collisions are based on the introduction of chromoelectric flux tube (strings) models [17], [18], [19]. String breaking mechanism approach is used for the conversion of the kinetic energy of a collision into field energy. Due to confinement, the color of these strings is restricted to a small area in transverse space. With increasing energy of the colliding particles, the number of strings grows and they start to overlap, forming clusters. This can introduce a possible dependence of particle production on the initial energy density and on the degree of collectivity achieved in collision processes at ultra-relativistic energies.

We focussed on the phenomenology and model calculations of heavy-ion reactions at LHC energies, extended also to ultra-high-energy proton-proton (pp) and proton-nucleus collisions (pA) [18], mainly to study possible Strong Colour Field (SCF) effects, as well as nuclear effects like shadowing and quenching embedded in our model. Theoretical predictions reported in [18] were obtained prior to LHC p+Pb runs (ALICE, CMS, ATLAS) at $\sqrt{s_{NN}}$ = 5 TeV.

<u>a. Predictions for p-Pb at 5.02A TeV for testing the nuclear shadowing in the initial state at LHC and comparison with experimental data</u>

The Monte Carlo type models HIJING1.0, HIJING2.0 and HIJING/BB2.0 were developed to study the production of hadrons in pp, p-A and A-A collisions. They are essentially two component models which describe the “hard” and “soft” processes. The jet production is calculated using the collinear factorized multiple minijet in pQCD. A p0 cut has to be introduced in the average transverse momentum resulted after the final jet production, bellow which value the interaction is considered non-perturbative and is characterized by the partonic “soft” cross section. The nucleon residues interact via “soft” gluons exchange described in string models. The pair of produced “hard” jets and the two excited residues are treated as independent strings which fragment in resonances which de-excite in the final hadrons. The string fragmentations in jets strongly depend on the string tension values. In HIJING 1.0 and HIJING2.0 a constant for the effective value of the string tension, k_0=1.0 GeV/fm is used. At high initial incident energy the new nuclear physics is due to the possibility of superposition of the longitudinal multiple flux tube which leads to strong effects of the longitudinal color field. The effects of the strong color field are modeled in HIJING/BB2.0 by varying the value of the effective string tensions. In order to describe the pp collisions and central Pb-Pb data at LHC it was shown that an energy and mass dependence of the string tension average value has to be considered. All the HIJING type models implement nuclear effects as the nuclear modification of the partonic distribution functions, that is “shadowing” and “jet quenching” through an induced parton breakage process in medium. While in the first two models a constant cut p_0=2 GeV/c and a “soft” partonic cross section σ_{soft}=54 mb are used, in HIJINGBB2.0 for A-A collisions a dependence on energy and mass of the cut parameter $p_0(s,A)$ was introduced at the RHIC and LHC energies for not violating the geometric limit of the total number of minijets on transverse area unit. One of the main

uncertainties in the charged particle multiplicity density calculation in Pb-Pb collisions is the nuclear modification of the partonic distribution functions, especially the low x gluon distributions. In the HIJING type models it is assumed that the parton distributions in a nucleus are factorized in a parton distribution in nucleon and the partonic shadowing factor. In the present calculations it is assumed that the shadowing effect for gluons and quarks is the same and the QCD evolution is neglected. Estimations of $dN_{ch}/d\eta$ and R_{pPb} as a function of pseudorapidity and of $(1/2\pi p_T)d^2N_{ch}/dp_T d\eta$ and R_{pPb} as a function of p_T for $|\eta|<0.8$ for minimum bias and 0-20% centrality (Fig. 35 and 36) in the p-Pb collision at 5.02 TeV were obtained.

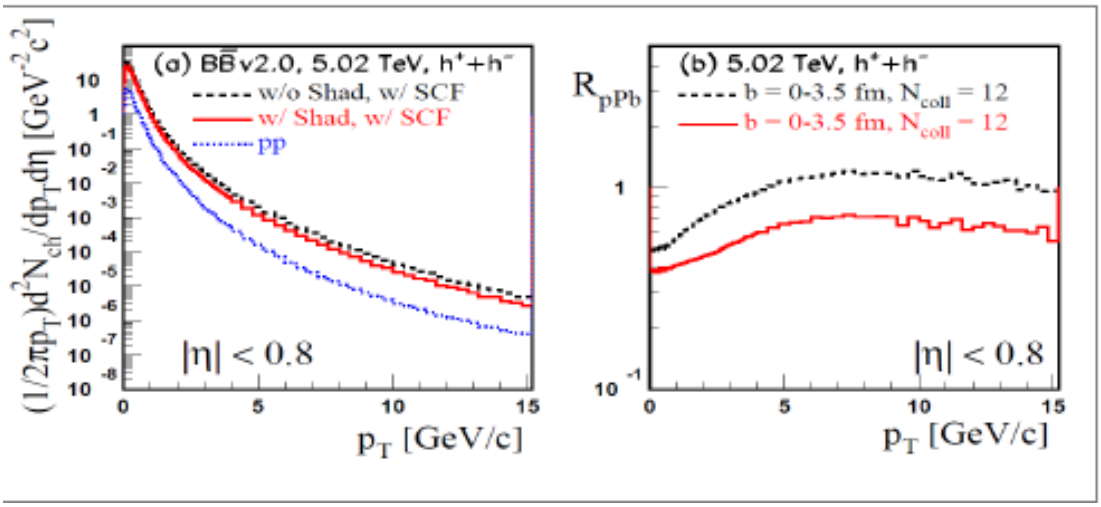

Fig. 35

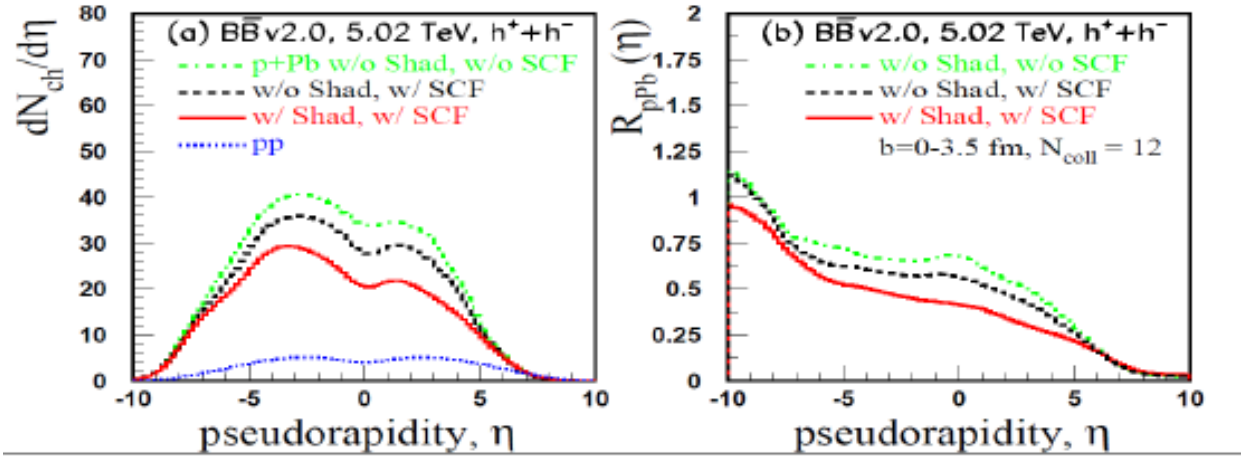

Fig. 36

Thus, even with a small sample of 10^6 events by studying $R_{pPb}(p_T)$ or the central relative to peripheral nuclear modification factor ($R_{CP}(pT)$) a definite constraint on the nuclear shadowing implemented in different models inspired by pQCD and saturation CGC models, with a large impact on the interpretation of results obtained in nucleus-nucleus collisions (Pb-Pb) at the LHC energies, can be given.

Theoretical results are presented in comparison with currently available data (ALICE, CMS, ATLAS) [20]. The calculations shown here have been updated by considering the same experimental cuts as the data. The experimental observables include multiplicity distributions, transverse momentum distribution, average transverse momentum, nuclear modification factor

R_{pPb} , forward and backward asymmetry. The detailed discussions of new results and conclusions are found in [20]. Moreover, comparison with data and other model calculations are also included. Note, the reference [20] is submitted to Int. J. Mod. Phys. E .

b. Study of Non-Perturbative Particle Production in Strong Colour Fields. Collective Effects and Their Dependence on Multiplicity at LHC energies

Effects of strong longitudinal colour electric fields (SCF), on the production of particles in nucleus-nucleus (Pb + Pb), proton-nucleus (p + Pb) and proton-proton (p + p) collisions were studied based on HIJING model and especially the new version (v2.0) of the HIJING/*BB* developed by us to simulate heavy ion collisions at ultra-relativistic energies. Here we focus our analysis at two energies of interest: √s= 0.9 TeV and √s= 7 TeV, where data for charged particles and identified particles (ID) have been reported for minimum bias (MB) events. The model calculations including SLCF effects give a good description of the spectral shape at low p_T (p_T <4 GeV/c) for both energies. At high p_T (p_T > 5 GeV/c) the calculations lead to a somewhat harder spectrum than that observed. In our phenomenology this could indicate that jet quenching, i.e., suppression of high p_T particles like that observed at RHIC energies in nucleus-nucleus collisions, could also appear in p+p collisions, particularly for events with large multiplicity [21]. Figure 37 compares the ALICE results to the predicted mid-rapidity spectra for positive pions (solid histograms), kaons (dashed histograms), and protons (dotted histograms) in minimum bias p+p collisions.
There is agreement in the p_T region of interest $1 < p_T < 4$ GeV/c at both energies. The over-prediction for proton and kaon production below p_T = 1 GeV/c is consistent with possible presence of radial flow, which seems to be larger at 7 TeV than at 0.9 TeV. The radial flow could appear as a consequence of a hydrodynamic type evolution with flux tube initial conditions [22], not embedded in our model.

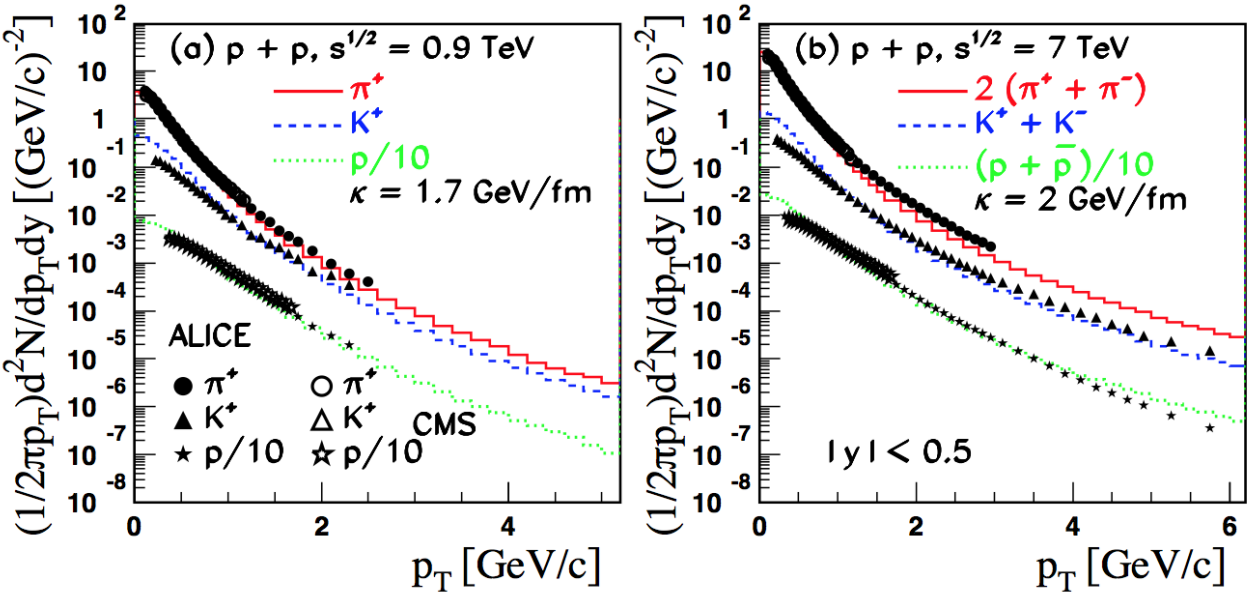

Fig. 37

We extend our analysis to the production of (multi)strange baryons. In Fig. 38 we show the HIJING/BB v2.0 model predictions of p_T spectra at mid-rapidity ($|y| < 0.5$) for Λ (solid histograms), Ξ^- (dashed histograms) and Ω^- (dotted histograms) baryons at 0.9 TeV and 7 TeV. For (multi)strange particles, the data indicate a stronger radial flow at 7 TeV than at 0.9 TeV. For the p_T region of interest, 1 < pT < 4 GeV/c, the model results are in agreement with data at both energies.

The ALICE Collaboration has reported measurements of the transverse momentum distribution of prompt open charmed mesons (D^0, D^+ , D^{*+} , $D_S{}^+$) in p + p collisions at √s= 7 TeV [23,24], and of (D^0, D^+, D^{*+}) at √s = 2.76 TeV [25] in the central rapidity range $|y| \leq 0.5$. Prompt indicates D mesons produced at the p + p interaction point, either directly in the hadronization of the charm quark or in strong decay of excited charm resonances. The contribution from weak decays of beauty mesons, which give rise to feed-down D mesons, were subtracted. The model calculations include SCF effects [19]. The energy dependence of string tension $\kappa(s) = \kappa_0 (s/s_0)^{0.04}$ GeV/fm, predict a modest increase when going from √s = 2.76 TeV (κ = 1.88 GeV/fm) to √s = 7 TeV (κ = 2.03 GeV/fm). Therefore, to calculate prompt open charmed mesons production we consider the same value of average string tension for charm and strange quark, i.e, $\kappa_C = \kappa_S \approx 2$ GeV/fm. The theoretical results are compared to data in Fig. 39. Predictions for $D_S{}^+$ mesons at √s =2.76 TeV are also included. The agreement between theory and experiment is good within experimental uncertainties, except at √s = 7 TeV where while the average cross section is well reproduced the predicted spectrum has a somewhat shallower slope than the data.

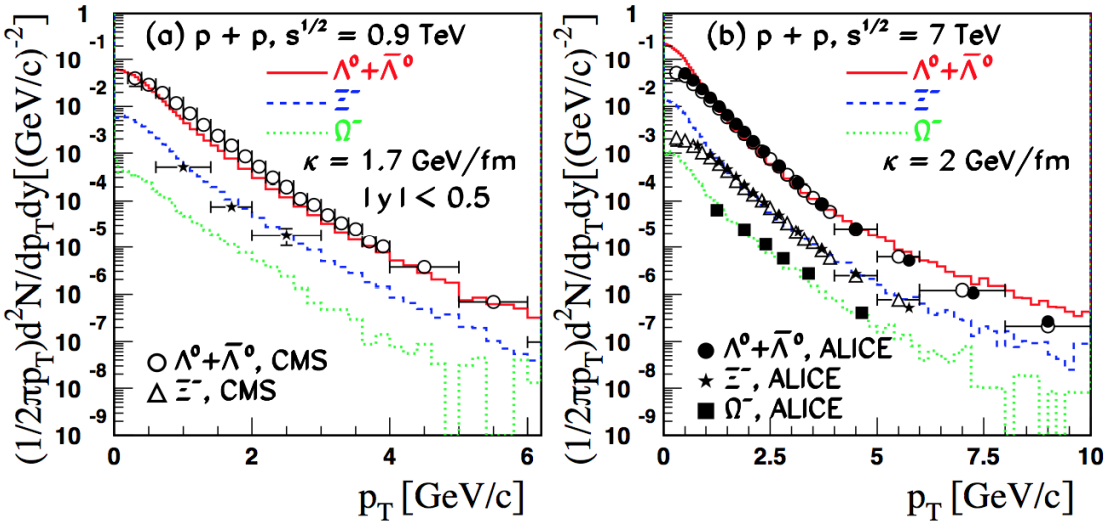

Fig. 38

The average transverse momenta as function of charged particle multiplicity ($<p_T>(N_{ch})$) are shown in Fig. 40 for pp collisions at √s = 7 TeV in comparison with ALICE data. It seems that mean charged particle as global observable is not a sensitive observable for SCF effects, and the data are well described with $\kappa = \kappa_0 = 1$ GeV/fm. The $< p_T > (N_{ch})$ of identifed particles (ID), i.e. $\pi^+ + \pi^-$, $K^+ + K^-$, p + pbar, $\Xi^+ + \Xi^-$, $\Omega^- + \Omega^+$) are shown in Fig. 41. The average transverse momentum of ID particle is more sensitive to the collective expansion. A model calculation for $< p_T >$ as function of multiplicity for various hadron species show that the change in the shape of the value of < pT > due to the transverse expansion is dependent on the individual hadron species of different mass. While the protons gain most in $< p_T >$, the pions loose some $< p_T >$. Therefore, the protons experience large flow-effect and could not be described by our model calculations.

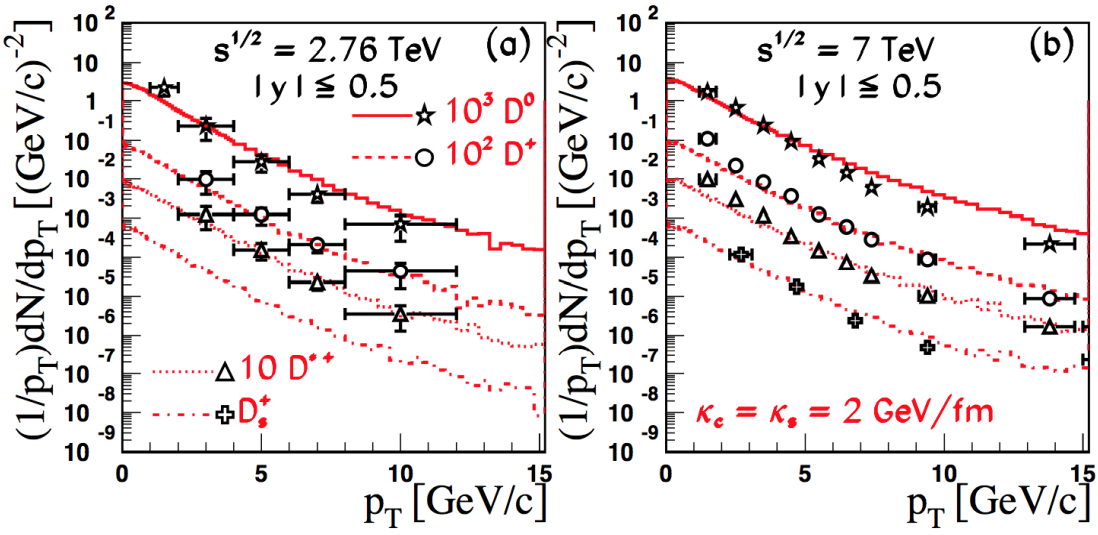

Fig. 39

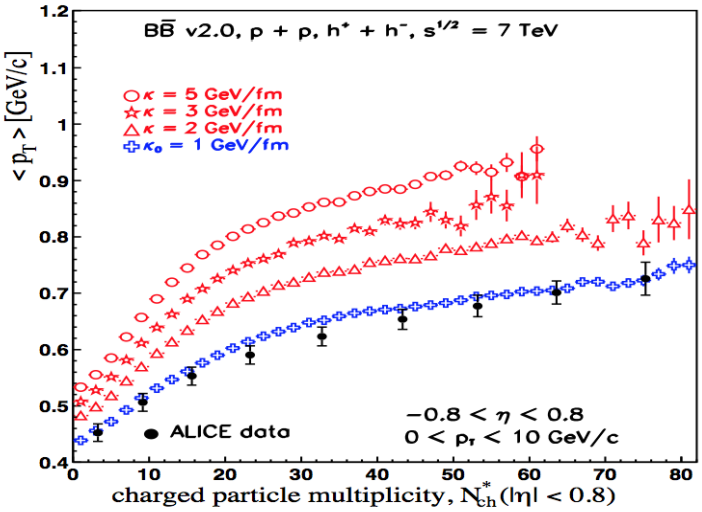

Fig. 40

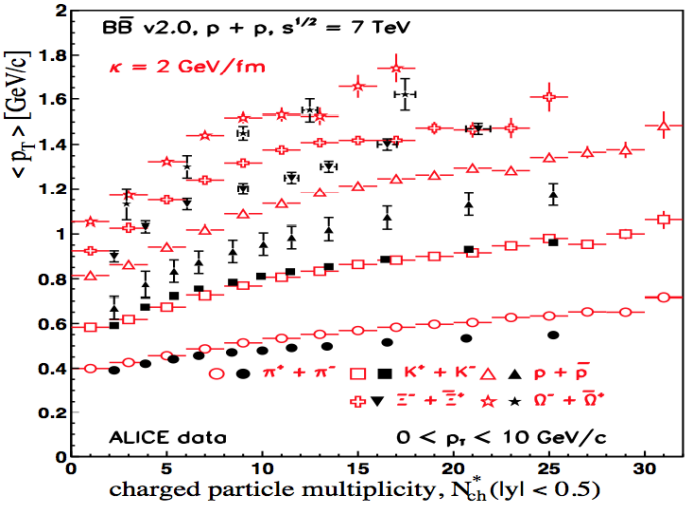

Fig. 41

Figure 42 present the model predictions of < pT > (Nch) for p + Pb collisions at 5.02 TeV. The calculations include SCF effects and JJ loops. The model predict a mass hierarchy and this fact could be quantitatively understood in hydrodynamics. For ID particles the < pT > in p + Pb collisions at √sNN = 5.02 TeV increases with multiplicity, at a rate which is stronger for heavier particles.

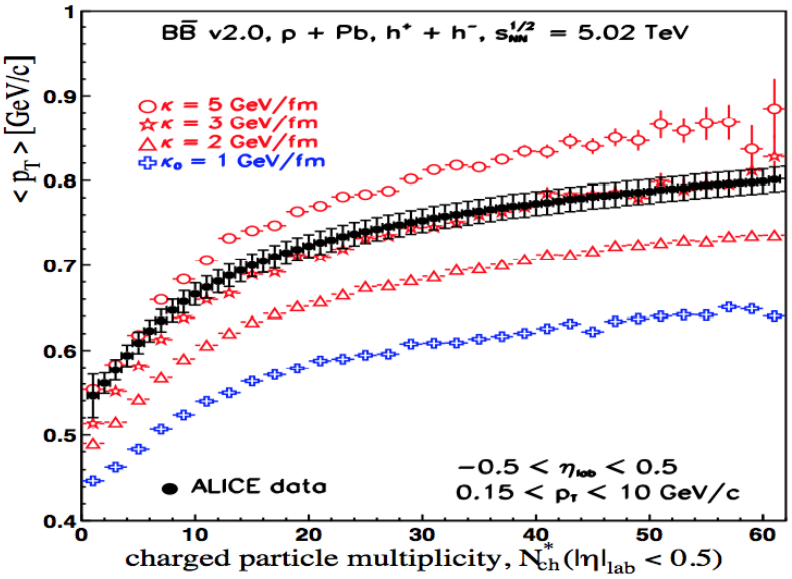

Fig. 42

This HIJING model based work is supported by the Natural Sciences and Engineering Research Council of Canada and by the Romanian Authority for Scientific Research, CNCS-UEFISCDI project number PN-II-ID-2011-3-0368.

2. Comparison of experimental results for pp collisions at √s = 7 TeV with the EPOS model

EPOS in its initial version was a sophisticated multiple scattering approach based on partons and Pomerons (parton ladders), with special emphasis on high parton densities. The latter aspect, particularly important in proton-nucleus or nucleus-nucleus collisions, is taken care of via an effective treatment of Pomeron-Pomeron interactions, referred to as parton ladder splitting. In addition, collective effects are introduced after separating the high density central core from the peripheral corona. EPOS is the successor of the NEXUS model.
The EPOS3 approach provides within a unique theoretical scheme the initial conditions for a hydrodynamical evolution in p-p, p-A, and HI collisions. The initial conditions are generated in the Gribov-Regge multiple scattering framework. An individual scattering is referred to as Pomeron, identified with a parton ladder, eventually showing up as flux tubes (also called strings). Each parton ladder is composed of a perturbative QCD (pQCD) hard process, plus initial- and final-state linear parton emission. The formalism is referred to as “parton-based Gribov Regge theory” and described in detail in Ref. [26]. Based on these initial conditions, ideal hydrodynamical calculations to analyze HI and p-p scattering at the BNL Relativistic Heavy Ion Collider (RHIC) and CERN Large Hadron Collider (LHC) have been performed. In [27] two major improvements: a more sophisticated treatment of nonlinear effects in the parton evolution by considering individual (per Pomeron) saturation scales and a 3D + 1 viscous hydrodynamical evolution were implemented. There are also changes in the core-corona procedure, which amounts to separation of the initial energy of the flux tubes into a part which constitutes the initial conditions for hydro (core) and the particles which leave the “matter.” This is crucial in all

collision types.
As a consequence of the rescaling due to collective flows, and in particular the radial flow, the number of secondary particles produced by the clusters is reduced. In case of a consistent treatment of cross-section and particle production like in EPOS, this property is needed in the case of HI collisions where less particles are observed than produced by the model without final state interactions. And indeed a proper hydro treatment like in EPOS 2 or 3 requires a large multiplicity in the initial state to finish with the correct multiplicity after a long evolution of the large volume of the core. But in the case of light system, like pp, using EPOS 2 or 3 with a realistic treatment of the hydrodynamical evolution with proper hadronization such an effect was not observed. In that case the large flow comes from the quick expansion of the very small volume of the core. As a consequence, in EPOS LHC [28] a different type of radial flow in case of very dense system in a small volume (where the critical energy density is reached because of multiple scattering between partons in a single pair of nucleons like in pp) was introduced. For this pp flow, characterized by the maximal radial rapidity y_{rad}, the mass of the cluster M is not changed before hadronization (multiplicity is conserved) but the energy conservation is imposed by a simple rescaling of the total momentum P (larger p_T are compensated by smaller p_z) after the radial boost. Of course a smooth transition is needed between the two kinds of system and the transition is observed in p-A interactions.
EPOS LHC and EPOS3 codes have been implemented in our group. The p_T distributions for pions, kaons and protons in pp collisions at √s =7 TeV have been compared with both versions of the models for MB and all the multiplicity bins. An example of this comparison can be followed in Fig. 43. As a conclusion the EPOS LHC version provides a slightly better overall description of the data as compared to EPOS3 version. Nevertheless, very accurate final experimental distributions obtained by us and the comparison with theoretical predictions will contribute to the refinement of the EPOS3 model based on hydrodynamical calculations and to the answer of the question: Do we see collective radial flow in pp collisions at LHC?

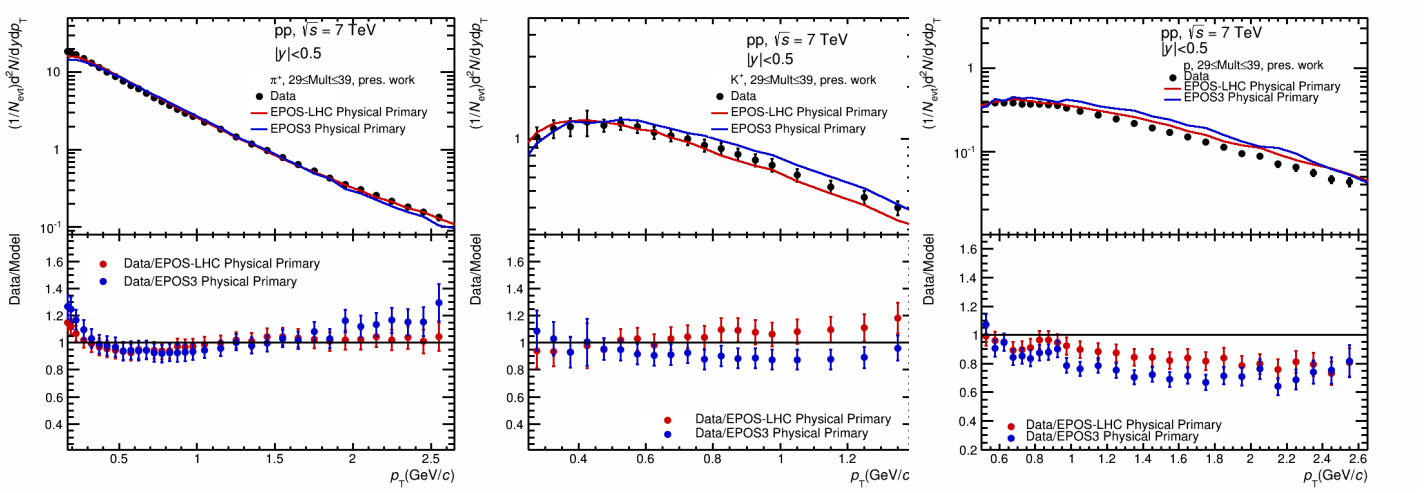

Fig. 43

In the time period of the project, presented in this report, our group had more than 45 presentations in different Working Groups of the ALICE Collaboration, Internal Notes of the ALICE Collaboration were edited, we are co-authors to more than 130 papers published in ISI journals and more than 35 presentations at International Conferences, their list being included in the project data basis.

References

1. ALICE Collaboration, C. Andrei et al. Nucl. Phys. A 20024, S0375-9474(14)00251-6:10.1016/j.nuclphysa.2014.08.002,Quark Matter 2014.
2. ALICE Collaboration, B. Abelev et al. Phys. Lett. B, 728:25, 2014.
3. E. Schnedermann et al. Phys. Rev. C, 48:2462, 1993.
4. R. Corke and T. Sjostrand. JHEP, 1001:35, 2010.
5. STAR Collaboration, L. Kumar, Quark Matter 2014.
6. ALICE Collaboration, B. Abelev et al. Phys. Rev. C, 88:044910, 2013.
7. P. Beckmann et al., Collective Azimuthal Alignment in Relativistic Heavy Ion Reactions, Mod. Phys. Lett. A 2, 163 (1987)
8. J. P. Alard and the FOPI Collaboration, Midrapidity source of intermediate-mass fragments in highly central collisions of Au + Au at 150A MeV, Phys. Rev. Lett. 69 (1992) 889.
9. S. Brandt, Ch. Peyrou, R. Sosnowski and A. Wroblewski, The principal axis of jets – an attempt to analyse high-energy collisions as two-body processes, Phys. Lett. 12 (1964) 57
10. E. Fahri, Phys. Quantum Chromodynamics Test for Jets, Rev. Lett. 39 (1977) 1587
11. J.D. Bjorken and S.J. Brodsky, Statistical Model for Electron-Positron Annihilation into Hadrons, Phys. Rev. D1 (1970) 1416
12. A. Banfi, Resummed event shapes at hadron-hadron colliders, JHEP 0408 (2004) 062, arXiv:hep-ph/0407287v3
13. G.C. Fox and S. Wolfram, Event shapes in e+ e− annihilation, Nucl. Phys. B149 (1979) 413. Nucl. Phys. B149 (1979) 413.
14. A. Herghelegiu, PhD Thesis, University of Bucharest
15. C. Andrei, PhD Thesis, University of Bucharest
16. Cristian Andrei, Ionela Berceanu, Alexandru Bercuci, Andrei Herghelegiu, Francesco Noferini, Mihai Petrovici, and Amalia Pop. Transverse momentum distributions of pions, kaons an pro- tons for high multiplicity and close to azimuthal isotropic events in 7 tev pp collisions with the alice experiment at the lhc (short analysis note based on the previous notes and presentations). Internal Note, April 2012. https://twiki.cern.ch/twiki/pub/ALICE/PWGLFPAGSPECTRAMultiplicityEventShapePP7/coll_ph_pp_ALICE_internal_note_310111.pdf. 91
17. Topor Pop V,Gyulassy M,Barrette J,Gale C, and Warburton A, Phys. Rev.C 86, 044902 (2012).
18. Albacete J L,M. Petrovici, V. Topor Pop, Int. J. Mod.Phys. E Vol. 22, 1330007 (2013).
19. V.T. Pop, M.Gyulassy, J.Barrette, C.Gale and M.Petrovici, J.Phys. G 41, 115101 (2014).
20. J.L.Albacete, M. Petrovici, V. Topor Pop et al., arXiv:1605.09479 [hep-ph]., submitted to Int. J. Mod. Phys. E
21. Abelev B et al (ALICE Collaboration), Phys. Rev. Lett. 110 032301 (2013)
22. K. Werner, I. Karpenko, T. Pierog, M. Bleicher and K. Mikhailov, Phys. Rev. C 83, 044915 (2011)
23. B. Abelev et al. [ALICE Collaboration], JHEP 1201, 128 (2012)
24. B. Abelev et al. [ALICE Collaboration], Phys. Lett. B 718, 279 (2012)
25. B. Abelev et al. [ALICE Collaboration], JHEP 1207, 191 (2012)
26. H. J. Drescher et al., Phys. Rep. 350:93, 2001.
27. K. Werner, B. Guiot, Yu. Karpenko, T. Pierog, Phys. Rev. C 89:064903, 2014.
28. T. Pierog et al., arXiv:1306.0121v2 [hep-ph] (2013) DESY-13-125.

Project leader,

Prof. Dr. Mihai Petrovici